Chapter 2
Description of Sim-CYCLE

2.1. Introduction

In this chapter, a comprehensive description of the new model, termed Sim-CYCLE (**Sim**ulation model of Carbon c**YC**le in Land **E**cosystems), is presented. Indeed, many models, which simulate the atmosphere-biosphere CO_2 exchange and carbon dynamics in global terrestrial ecosystems, have been constructed, as follows (see reviews by Cramer et al., 1999; Churkina et al., 1999; Bondeau et al., 1999; Kicklighter et al., 1999; Nemry et al. 1999; Ruimy et al., 1999; Schloss et al., 1999):

BIOME: Haxeltine and Prentice (1996), Haxeltine et al. (1996)

CARAIB: Warnant et al. (1994), François et al. (1996)

CASA: Potter (1999), Potter et al. (1993, 1998, 1999), Potter and Klooster (1997, 1998, 1999), DeFries et al. (1999)

CENTURY: Parton et al. (1988, 1993, 1994), Ojima et al. (1993), Schimel et al. (1994), Scurlock et al. (1999)

CEVSA: Cao and Woodward (1998a,b)

DEMETER: Foley (1994a,b, 1995a,b)

DOLY: Woodward et al. (1995)

FBM: Lüdeke et al. (1994, 1995, 1996), Kinderman et al. (1993, 1995), Hager et al. (1999)

GLO-PEM: Prince and Goward (1995)

HYBRID: Friend (1997)

IBIS: Foley et al. (1996), Delire and Foley (1999), Levis et al. (2000)

OBM (HRBM): Esser (1984, 1987, 1994, 1995), Esser et al. (1994)

PLAI: Plöchl and Cramer (1995)

QUEST: Gifford (1992, 1994)

SDBM: Knorr and Heimann (1995)

SILVAN: Kaduk and Heimann (1996)

SLAVE: Friedlingstein et al. (1994, 1995)

TEM: Raich et al. (1991), Melillo et al. (1993), McGuire et al. (1992, 1993, 1997), Xiao et al. (1998), Tian et al. (1998, 1999)

TURC: Ruimy et al. (1996a,b)

However, they have relatively simple structure and need a smaller number of parameters and input data. In contrast, those oriented to plot-scale simulations have generally complicated structure and need a large number of parameters, reducing their tractability, although they exhibit high accuracy (Rastetter et al., 1991; McMurtrie et al., 1992b; Kirschbaum, 1999). Exceptionally, the forest model FOREST-BGC (Running and Coughlan, 1988) was successfully applied to the global scale (BIOME-BGC: Runnig and Hunt, 1993; Hunt et al., 1996; Kimball et al., 1997; White et al., 1997); this may owe the utilization of remote sensing data. Therefore, Sim-CYCLE aims at success in global simulations using the climate projection by general circulation models (GCMs), and then is designed as a prognostic, process-based model driven by climatic variables, as detailed below. The code of Sim-CYCLE is written in C-language and executable on many platforms; the complete code is presented in Appendix A. When one conducts a global-scale simulation with Sim-CYCLE, using a high-performance workstation is strongly recommended, while a plot-scale simulation is readily executable by inexpensive personal computers.

2.2. Model description

2.2.1. Overview of ecosystem carbon dynamics

Sim-CYCLE is developed based on the ecosystem-scale model by Oikawa (1985), which has been used to simulate and analyze a tropical rain forest ecosystem (Oikawa, 1986a, 1987, 1989), temperate evergreen broad-leaved forest (Oikawa, 1998), and grassland (Oikawa,

1993; Alexandrov and Oikawa, 1995). Moreover, structural and functional changes in tropical rain forest in response to atmospheric CO_2 doubling were investigated with the model (Oikawa 1986b). The advantages of Sim-CYCLE are attributable to: (1) adoption of the dry-matter production theory, (2) mechanistic structure of carbon dynamics, (3) physiological regulation of carbon fluxes, and (4) intermediate complexity suitable for global simulations (these aspects will also be discussed in Chapter 7).

In Sim-CYCLE, terrestrial carbon dynamics is conceptualized as a five-compartment system (Fig. 2-1). Carbon in a given ecosystem (*WE*) is composed of the plant biomass (*WP*) and soil organic carbon (*WS*). *WP* is divided into three compartments, i.e. foliage (subscript *F*), stem and branch (subscript *C*), and root (subscript *R*); *WS* is divided into two compartments, i.e. litter (i.e. dead biomass; subscript *L*) and mineral soil (i.e. passive component of soil organic matter, e.g. humus; subscript *H*).

$$WE = WP + WS \tag{2-1a}$$

$$WP = WP_F + WP_C + WP_R \tag{2-1b}$$

$$WS = WS_L + WS_H \tag{2-1c}$$

The atmosphere-biosphere CO_2 exchange occurs through three major processes: gross photosynthetic production (*GPP*), autotrophic plant respiration (*AR*), and heterotrophic soil respiration (*HR*). The net primary production (*NPP*), defined as follows,

$$NPP = GPP - AR \tag{2-2}$$

indicates the net amount of plant dry-matter production, and is an important quantity not only for ecology but also for agronomy and forestry. The net ecosystem production (*NEP*), defined by the following,

$$NEP = NPP - HR \tag{2-3}$$

indicates the carbon balance of the ecosystem during a given period: a net sink or a source. Within a terrestrial ecosystem, carbon is transferred in various forms of organic compound (largely carbohydrate) through a couple of processes (Fig. 2-1), including translocation of photosynthate *PT*, litterfall of dead biomass *LF*, and synthesis of humic mineral soil *HF*. In this stage, we neglect animal processes and lateral transportation of carbon from one ecosystem to another. The net change in each compartment (Δ) during a given period is given by the followings:

$$\Delta WP_F = PT_F - ARG_F - LF_F \quad (2\text{-}4a)$$

$$\Delta WP_C = PT_C - ARG_C - LF_C \quad (2\text{-}4b)$$

$$\Delta WP_R = PT_R - ARG_R - LF_R \quad (2\text{-}4c)$$

$$\Delta WS_L = LF - HR_L - HF \quad (2\text{-}4d)$$

$$\Delta WS_H = HF - HR_H \quad (2\text{-}4e)$$

where the carbohydrate translocation *PT* is determined as the difference between *GPP* and *ARM* (see Section 2.4.5). Apparently, Δ*WE* is equal to *NEP*. Since in Sim-CYCLE these fluxes are calculated monthly, we can simulate seasonal, inter-annual, and successional behaviors of terrestrial carbon dynamics. As a result of simulation, we will acquire the estimations of such important quantities as plant biomass, soil carbon storage, leaf area index (*LAI*), *NPP*, and *NEP*.

2.2.2. Basic data and environmental condition

The basic data used in this study were derived from a couple of global datasets. Since the original data have coarse resolutions, we interpolated the data for the plot-scale simulation (i.e. 0.5°x0.5°). For the control climate (monthly), we chose a dataset by U.S. National Centers for Environmental Prediction and U.S. National Center for Atmospheric Research. This is one of the reanalysis products (Kalnay et al., 1996), hereafter termed the

NCEP/NCAR-reanalysis. We could obtain such climatic components as the ground surface temperature (*TG*), air temperature at 2 m height (*TA*), total precipitation (*PR*), mean cloudiness (*CL*), soil temperature at 10 cm and 200 cm depths (TS_{10} and TS_{200}), specific humidity at 2 m above the ground (*SHM*), and wind velocity (*WND*). The control climate condition was obtained by averaging for a sufficiently long term, from Jan. 1961 to Dec. 1998. For the soil condition, the rooting depth and water holding capacity (*WHC*) were derived from Webb et al. (1993), and hydraulic conductivity (*GH*) were from Zobler (1986). Using these primary data, we estimated more detailed ecosystem environments, such as day-length (*DL*), photosynthetic photon flux density (*PPFD*), net radiation (*RN*), evapotranspiration (*AET*), and soil water content (*MS*).

2.2.2.1. Radiation

Angular solar elevation above the horizontal (SE_{MD}) at any latitude and at any day of the year is formulated as follows (subscript *MD* indicates a value at midday)

$$\sin(SE_{MD}) = \sin(LAT)\cdot\sin(SLD) + \cos(LAT)\cdot\cos(SLD) \qquad (2\text{-}5)$$

where *LAT* is the site latitude ($-90^{\circ}_{(south)} \le LAT \le 90^{\circ}_{(north)}$) and *SLD* is the solar declination of the Earth's orbit ($-23.4^{\circ} \le SLD \le 23.4^{\circ}$). The term *SLD* is approximated by the following empirical equation:

$$SLD = 23.4\cdot\sin\left[55.7\left(ND - ND_{VE}\right)\right] \qquad (2\text{-}6)$$

where *ND* is the number of days from the beginning of the year ($0 \le ND \le 364$, neglecting leap years), and ND_{VD} represents the *ND* at the vernal equinox (ND_{VE}=80). Using these parameters, hour-angle from sunrise to midday *HA* and day-length *DL* are calculated as follows:

$$HA = \mathrm{acos}\left[-\tan(LAT)\tan(SLD)\right] \qquad (2\text{-}7)$$

$$DL = 24\left(1 - \frac{HA}{180}\right) \tag{2-8}$$

Figure 2-2 shows the calculated seasonal change in DL at different latitudes. Similarly, irradiance of solar radiation at the atmosphere-top at midday (RTT_{MD}) is derived from the following equation:

$$RTT_{MD} = SLC\left(\frac{ESD_0}{ESD}\right)^2 \sin(SE_{MD}) \tag{2-9}$$

where SLC denotes the solar constant (1365 W m^{-2}), ESD is the distance between the sun and the earth (ESD_0 represents the annual mean). The second part of Eq. 2-9, related to relative sun-earth distance, is given by the following:

$$\left(\frac{ESD_0}{ESD}\right)^2 = 1.000111 + 0.034221\cos(SA) + 0.00128\sin(SA) + 0.000719\cos(2SA) + 0.000077\sin(2SA) \tag{2-10}$$

where SA is the parameter of season, i.e. seasonal angle of the Earth's orbit (SA=360· ND/365).

In the atmosphere, the incident radiation RTT_{MD} is attenuated by airborne particles and clouds to the level of RTG_{MD} at the ground surface. The effect is empirically formulated as a function of cloudiness ($CL \leq 0.8$) by Iqubal (1983) (see Fig. 2-3), as follows:

$$\frac{RTG_{MD}}{RTT_{MD}} = 0.803 - 0.34CL - 0.458CL^2 \tag{2-11}$$

For example, when a quarter of the sky is covered with clouds (CL=0.25), RTG_{MD} is

attenuated to 69 % of RTT_{MD}. In addition to the attenuation effect on irradiance, scattering in the atmosphere optically alters the ratio between direct radiation and diffuse radiation; that is, a cloudy sky brings about a larger proportion of scattered radiation. The total solar radiation at the ground is divided into diffuse radiation (RFG_{MD}) and direct radiation (RDG_{MD}):

$$RFG_{MD} = RTG_{MD}\left(0.958 - 0.982\frac{RTG_{MD}}{RTT_{MD}}\right) \tag{2-12a}$$

$$RDG_{MD} = RTG_{MD} - RFG_{MD} \tag{2-12b}$$

Importantly, *RFG* and *RDG* differ in their fractional content of photosynthetically active radiation (PAR: 400-700 nm) in the total spectrum; *RDG* contains 43 % of PAR, while *RFG* contains 57 %. Then, photosynthetic photon flux density $PPFD_{MD}$ is given by the following:

$$PPFD_{MD} = 4.6 \cdot 0.43 \cdot RDG_{MD} + 4.2 \cdot 0.57 \cdot RFG_{MD} \tag{2-13}$$

where the multipliers 4.6 and 4.2 are for unit conversion from W m^{-2} to μ mol photons m^{-2} s^{-1} for direct and diffuse radiation, respectively (Larcher, 1995). Figure 2-4 shows the calculated seasonal change in $PPFD_{MD}$ (under clear sky) at different latitudes.

Net radiation, the energy input to ecosystem, is required for estimating the potential evapotranspiration rate based on the Penman-Monteith method (Monteith, 1981; described later). To estimate the evaporation rate from soil surface and the transpiration rate from canopy, canopy net radiation *RNP* and soil surface net radiation *RPS* are separated from the total net radiation *RN*, accounting for the interception by the canopy *IR*:

$$IR = \exp(-KA \cdot LAI) \tag{2-14}$$

where *KA* is the attenuation coefficient (cf. Eq. 2-51). The net radiation contains short-wave (subscript *ST*) and long-wave (subscript *LN*) components; e.g. $RNP=RNP_{ST}+RNP_{PL}$. The short-

wave terms are a function of incident solar radiation *RTS* and surface reflectance, or albedo: *ALP* for plant canopy, and *ALS* for soil surface.

$$RNP_{ST} = RTS \cdot IR\,(1 - ALP) \tag{2-15a}$$

$$RNS_{ST} = RTS\,(1 - IR)\,(1 - ALS) \tag{2-15b}$$

ALP differs among plant types (from 0.12 of conifers to 0.30 of herbs; Jones, 1992), while *ALS* is a function of snow accumulation (*SNA*) (see Fig. 2-5):

$$ALS = \alpha_1 + \frac{\alpha_2}{1 + \exp\left[-\alpha_3 (SNA - \alpha_4)\right]} \tag{2-16}$$

where α_1 to α_4 are the parameters. The seasonal change in surface albedo is important especially in northern ecosystems which have a seasonal snow cover. Finally, the net long wave radiation RN_{LN} is estimated by an empirical formula (Suzuki, 1992):

$$RN_{LN} = SBC(TA + ZAT)^4 \cdot F_{RN}(CL) \cdot F_{RN}(VPD) \tag{2-17}$$

where *SBC* is the Stefan-Boltzmann constant (5.67×10^{-8} W m^{-2} K^{-4}), *TA* is the air temperature, and *ZAT* is the absolute temperature at zero degree centigrade (=273.15 K). RN_{LN} is divided into RNP_{LN} and RNS_{LN} in a similar manner to Eq. 2-15. $F_{RN}(CL)$ and $F_{RN}(VPD)$ are empirical functions representing the controls of cloud and air humidity, respectively.

$$F_{RN}(CL) = 1 - 0.65CL \tag{2-18a}$$

$$F_{RN}(VPD) = 0.39 + \frac{0.058}{VPD} \tag{2-18b}$$

where *CL* is the cloudiness, and *VPD* is the vapor pressure deficit (Eq. 2-30).

2.2.2.2. Water budget

The water cycle in terrestrial ecosystems is simulated by a subscheme (Fig. 2-1) as simple as upper layer (MS_{UP}, from 0 to 30 cm depth), lower layer (MS_{LW}, from 30 cm to rooting depth), and snow accumulation (SNA). For each water component, net balance of water content (Δ) during a given period is represented as follows:

$$\Delta MS_{UP} = \left(PR_{RAIN} - IC\right) + TW - EV - PN \tag{2-19a}$$

$$\Delta MS_{LW} = PN - TR - RO \tag{2-19b}$$

$$\Delta SNA = PR_{SNOW} - TW \tag{2-19c}$$

where PR_{RAIN} and PR_{SNOW} are the rain and snow fractions of total precipitation (PR), respectively, PN is penetration from the upper to the lower layer, and RO is the subsurface runoff. The actual evapotranspiration is composed of evaporation (EV) from soil surface and transpiration (TR) from vegetation canopy. Here, we assumed that runoff and transpired water are subtracted from lower layer (MS_{LW}); this may not lead to a significant error in a monthly-step simulation. The fraction of snowfall in total precipitation is a function of air temperature TA: (Fig. 2-6)

$$\frac{PR_{SNOW}}{PR} = \frac{1}{1 + \exp\left[0.75(TA - 2)\right]} \tag{2-20}$$

For example, the PR_{SNOW} accounts for a half of PR at 2 °C. The thawing of snow (TW) is also a function of ground temperature TG:

$$TW = \frac{SNA}{1 + \exp(-0.375TG)} \tag{2-21}$$

The penetration of gravity water from the upper to the lower layer is a function of the water input to the upper layer and the hydraulic conductivity (*GH*):

$$PN = GH\left(PR_{RAIN} + TW\right) \tag{2-22}$$

$$IC = 0.02\ LAI \cdot PR_{RAIN} \tag{2-23}$$

In this model, upward movement of capillary water under a dry condition is neglected. The runoff from lower layer is parameterized by using a simple equation of the Bucket model (Manabe, 1969):

$$RO = \sqrt[3]{RF^3 + DI^3} - DI \tag{2-24a}$$

$$DI = WHC - MS_{LW} \tag{2-24b}$$

where *DI* denotes the dryness index, and *WHC* is the soil water holding capacity. The potential evaporation (EV_{PM}) and transpiration (TR_{PM}) are estimated by the Penman-Monteith method, assuming an abundant water supply.

$$EV_{PM} = \frac{SLVP_{SAT} \cdot RNG + AD \cdot ASH \cdot VPD \cdot GG}{LH\left[SLVP_{SAT} + PSC(GG/GA)\right]} \tag{2-25a}$$

$$TR_{PM} = \frac{SLVP_{SAT} \cdot RNC + AD \cdot ASH \cdot VPD \cdot GS}{LH\left[SLVP_{SAT} + PSC(GS/GA)\right]} \tag{2-25b}$$

where *AD* is the air density, *ASH* is the specific heat of air, *LH* is the latent heat of vaporization (2.5 MJ kg^{-1} H_2O), and *PSC* is the psychrometer constant (0.667 Pa K^{-1}). The term $SLVP_{SAT}$ is the slope of saturated vapor pressure which is a function of temperature, and *VPD* is the vapor pressure deficit.

$$SLVP_{SAT} = \frac{6.1078 \cdot \beta_1}{0.4615(TA + ZAT)} 10^{\frac{\beta_2 \cdot TA}{\beta_3 + TA}} \quad (2\text{-}26)$$

$$VP_{SAT} = 6.1078 \cdot 10^{\frac{\beta_2 \cdot TA}{\beta_3 + TA}} \quad (2\text{-}27)$$

The parameters β_1 to β_3 are dependent on temperature conditions. If TA>0 °C:

$$\beta_1 = 2500 - 2.4TA, \ \beta_2 = 7.5, \ \beta_3 = 273.3 \quad (2\text{-}28a)$$

otherwise:

$$\beta_1 = 2834, \ \beta_2 = 9.5, \ \beta_3 = 265.3 \quad (2\text{-}28b)$$

Consequently, VP and VPD are respectively given by the followings:

$$VP = \frac{AP \cdot SHM}{0.622 + SHM} \quad (2\text{-}29)$$

$$VPD = VP_{SAT} - VP \quad (2\text{-}30)$$

where SHM is the specific humidity. The term AD in Eq. 2-25 is the air density, which is a function of temperature (TA), vapor pressure (VP), and air pressure (AP):

$$AD = 1.293 \frac{ZAT}{TA + ZAT} \frac{AP}{AP_0} \left(1 - 0.378 \frac{VP}{AP}\right) \quad (2\text{-}31)$$

$$\frac{AP}{AP_0} = \exp\left[\frac{-283.8962ALT}{UGC(TA + ZAT)}\right] \quad (2\text{-}32)$$

where AP_0 is the control air pressure at the sea-level at 15°C (1013.25 hPa), UGC is the

universal gas constant (8.3144 J mol^{-1} K^{-1}), and *ALT* is the altitude of the site. The *GA* and *GG* denote the aerodynamic conductance and ground conductance for water vapor, respectively:

$$GA = \frac{KC^2 \cdot WND}{[\log(HT)]^2} \tag{2-33}$$

$$GG = GG_0\left(\frac{MS_{LW}}{WHC}\right) \tag{2-34}$$

where *KC* is the von Karman's constant (0.41), *WND* is the wind velocity at the height of *HT*, and GG_0 is the water-saturated conductance (i.e. the evaporative surface is at the soil surface). The canopy conductance *GC* is the integral of single-leaf conductance *GS*, which is a function of assimilation rate and then changes vertically in the canopy. The daily mean *GC* is obtained in a similar manner to daily *GPP* (cf. Eq. 2-55).

$$\begin{aligned} GC &= \frac{\int_0^{DLLAI}\int_0^{DL} GS\, dLAI\, dt}{DL} \\ &= \frac{2GS_{SAT}}{KA}\left[\ln\left\{1+\sqrt{1+KA\cdot SLGS\cdot PPFD_{MD}/GS_{SAT}}\right\}\right. \\ &\quad \left. -\ln\left\{1+\sqrt{1+KA\cdot SLGS\cdot PPFD_{MD}\cdot\exp(-KA\cdot LAI)/GS_{SAT}}\right\}\right] \end{aligned} \tag{2-35}$$

where GS_{SAT} is the light-saturated stomatal conductance, and *SLGS* is the initial slope of the *PPFD-GS* curve (derived from Eq. 2-42). Due to the limitation of water availability, evapotranspiration rates are reduced from the potential values, EV_{PM} and TR_{PM}, to the actual values, *EV* and *TR*, as approximated by a quadratic function:

$$CV\cdot EV^2 - (MS_{UP} + EV_{PM})EV + MS_{UP}\cdot EV_{PM} = 0 \tag{2-36a}$$

$$CV\cdot TR^2 - (MS_{LW} + TR_{PM})TR + MS_{LW}\cdot TR_{PM} = 0 \tag{2-36b}$$

where CV is the convexity of the MS_{UP}-EV and MS_{LW}-TR curves. As a solution of these equations, actual evaporation and transpiration rates are respectively given (see Fig. 2-7):

$$EV = \frac{(MS_{UP} + EV_{PM}) - \sqrt{(MS_{UP} + EV_{PM})^2 - 4CV \cdot MS_{UP} \cdot EV_{PM}}}{2CV} \quad (2\text{-}37a)$$

$$TR = \frac{(MS_{LW} + TR_{PM}) - \sqrt{(MS_{LW} + TR_{PM})^2 - 4CV \cdot MS_{LW} \cdot TR_{PM}}}{2CV} \quad (2\text{-}37b)$$

The potential and actual evapotranspiration rates (PET and AET, respectively) are frequently used in considering the ecosystem water use:

$$PET = EV_{PM} + TR_{PM} + IC \quad (2\text{-}38a)$$

$$AET = EV + TR + IC \quad (2\text{-}38b)$$

because they are closely related to the hydrological state of the ecosystem and plant water-use efficiency as a result of canopy gas-exchange.

2.2.3. Single-leaf processes

As shown in Fig. 2-8, single-leaf gas exchange is the most fundamental process for plant ecophysiology, which has investigated the controls of various environmental factors on stomata, the vent of photosynthesis and transpiration. The controls are described at the physiological scale and extended to the canopy scale (cf. the next section). The single-leaf photosynthetic rate (PC) is formulated as a Michaelis-type function of the incident PAR irradiance $PPFD_{IN}$ (Tamiya, 1951; Fig. 2-9), given by:

$$PC = \frac{PC_{SAT} \cdot QE \cdot PPFD_{IN}}{PC_{SAT} + QE \cdot PPFD_{IN}} \quad (2\text{-}39)$$

where PC_{SAT} is the single-leaf photosynthetic rate under light-saturation, and QE is the light-use efficiency, or quantum yield of photosynthesis. The terms PC_{SAT} and QE are complicated functions of temperature, CO_2 level, air humidity, and soil water, and are different among biome types and between C_3 and C_4 species (principal differences between C_3 and C_4 plants are listed in Table 2-1). They are formulated by using coefficient functions of important environmental factors, in a multiplicative way:

$$QE = QE_0 \cdot F_{QE}(TG) \cdot F_{QE}(CD_{ICL}) \tag{2-40}$$

$$PC_{SAT} = PC_{SAT0} \cdot F_{PC}(TG) \cdot F_{PC}(CD_{ICL}) \cdot F_{PC}(SW_L) \tag{2-41}$$

where QE_0 and PC_{SAT0} are respectively the potential maximum values under the optimal condition of QE and PC, and the terms F_{QE}()s and F_{PC}()s denote the coefficient functions of temperature, CO_2, and water conditions. Before describing these coefficient functions, we explain the regulation of single-leaf gas exchange through stomatal conductance (GS), at first. Sim-CYCLE adopts a semi-empirical model of stomatal conductance (Ball et al., 1987) modified by Leuning (1990), given by the following:

$$GS = \chi_1 + \frac{\chi_2 \cdot PC}{(CD_{ATM} - CD_{CMP})(1 + VPD / \chi_3)} \tag{2-42}$$

where CD_{ATM} is the atmospheric CO_2 concentration, VPD is the vapor pressure deficit, CD_{CMP} is the CO_2 compensation point of photosynthesis, and χ_1 to χ_3 are the biome-specific parameters, respectively. Equation 2-42 suggests that GS decreased as increasing atmospheric CO_2 concentration (Fig. 2-10), which is the case in many observations (Morison and Gifford, 1983; Field et al., 1995a). Since gas exchange through leaf epidermal cuticular is negligible (Nobel, 1999), the leaf intercellular CO_2 concentration CD_{ICL} is defined as follows (Fig. 2-11):

$$CD_{ICL} = CD_{ATM} - \frac{PC}{GS/1.56} \tag{2-43}$$

where CD_{ICL} is the intercellular CO_2 concentration. The CD_{ICL}, rather than CD_{ATM}, is related to the photosynthetic capacity, although CD_{ICL} tends to be parallel with the CD_{ATM}.

As with the photosynthetic quantum yield QE, Ehleringer and Pearcy (1977) revealed that C_3 and C_4 species respond to temperature and CO_2 conditions in disparate manners. Typically, QE of C_4 species is virtually insensitive to surrounding condition (i.e. $F_{QE}(TG)= F_{QE}(CD_{ICL})=1$), because of their CO_2 condensation mechanism eliminating photorespiration. In contrast, as shown in Figs. 2-12 and 2-13, QE of C_3 species depends strongly on temperature (TG) and CO_2 level (CD_{ICL}):

$$F_{QE}(TG) = \frac{52 - TG}{3.5 + 0.75(52 - TG)} \tag{2-44a}$$

$$F_{QE}(CD_{ICL}) = \frac{CD_{ICL}}{90 + 0.6CD_{ICL}} \tag{2-44b}$$

Ehleringer et al. (1997) suggest that the difference in QE between C_3 and C_4 species may be so important that it determines the geographical distribution of these two plant types.

Moreover, it is fully recognized that PC_{SAT} of C_4 species is much higher than C_3 species, and that C_4-photosynthesis is vulnerable to low temperatures. Sim-CYCLE incorporates such findings into the corresponding coefficient functions. The temperature dependence of PC_{SAT} depicts a bell-shape curve, and is formulated (Raich et al., 1991) as follows (Fig. 2-14):

$$F_{PC}(TG) = \frac{(TG - T_{MAX})(TG - T_{MIN})}{(TG - T_{MAX})(TG - T_{MIN}) - (TG - T_{OPT})^2} \tag{2-45}$$

where T_{MAX}, T_{MIN}, and T_{OPT} are respectively the maximum, minimum, and optimum temperatures for photosynthesis. For C_3 plants, T_{OPT} is a function of intercellular CO_2 concentration (Berry and Björkman, 1980; Kirschbaum and Farquhar, 1984; Fig. 2-15):

$$T_{OPT} = T_{OPT0} + 0.01\ CD_{ICL} \tag{2-46}$$

Equations 2-43 and 2-45 indicate that influences of atmospheric CO_2 rise and temperature rise may be interactive, making it difficult to predict even at the physiological scale, as demonstrated by a biochemical model study (Long, 1991). The CO_2 dependence of PC_{SAT} is expressed by a Michaelis-type function (Fig. 2-16):

$$F_{PC}(CD_{ICL}) = \frac{CD_{ICL} - CD_{CMP}}{KM_{CD} + CD_{ICL}} \tag{2-47}$$

where KM_{CD} is a parameter. CD_{CMP} differs largely between C_3 and C_4 species; C_4 species have a very low and constant CD_{CMP} (e.g. 5 ppmv), while C_3 species have higher and variable CD_{CMP}. Brooks and Farquhar (1985) formulated the CD_{CMP} of C_3 species as a function of temperature (Fig. 2-17):

$$CD_{CMP} = CD_{CMP0}\left[1 + \delta_1(TG - 20) + \delta_2(TG - 20)^2\right] \tag{2-48}$$

where CD_{CMP0} is the control value at 20 °C, and δ_1 and δ_2 are parameters. Apparently, $F_{PC}(CD_{ICL})$ represents the stomatal limitation of water stress on photosynthesis, because CD_{ICL} is strongly regulated by stomatal conductance which responds to air humidity (cf. Eqs. 2-42 & 2-43). On the other hand, $F_{PC}(MS_{LW})$ indicates the non-stomatal limitation of water stress (Tenhunen et al., 1984; Jones, 1985), that is, the direct effect of soil water availability on photosynthetic capacity:

$$F_{PC}(MS_{LW}) = \frac{MS_{LW}}{KM_{SW} + MS_{LW}} \quad (2\text{-}49)$$

where KM_{SW} is a parameter representing the sensitivity. Since the components of single-leaf gas exchange, i.e. GS, CD_{ICL}, PC, and QE, change interactively, a stationary state is numerically found by iterative calculation from Eq. 2-39 to Eq. 2-49.

2.2.4. Ecosystem-scale processes

2.2.4.1. Photosynthesis

GPP is the ultimate origin of all organic carbon in an ecosystem, where atmospheric CO_2 is fixed into dry matter (Terashima and Hikosaka, 1995). It is assumed the environmental factors except for PAR irradiance, i.e. temperature, CO_2, and water, should be similar among all leaves.

Indeed, the scaling procedure in terms of *GPP* is one of the characteristics of Sim-CYCLE, such that *GPP* is estimated by the dry-matter production theory established by Monsi and Saeki (1953). They firstly formulated the downward attenuation of PAR irradiance due to mutual shading of leaves in a canopy with accumulating leaf area, given by the following (Fig. 2-19):

$$PPFD_{IN} = PPFD_{TOP} \exp(-KA \cdot LAI_{CML}) \quad (2\text{-}50)$$

where $PPFD_{TOP}$ denotes the incident PAR at the canopy-top. Apparently, it attenuates exponentially with the biome-specific coefficient KA, such that a leaf underlying the cumulative leaf area index LAI_{CML} receives the light of $PPFD_{IN}$. We assume the spherical distribution of leaf inclination, and then the term KA is a function of solar height (Kuroiwa and Monsi, 1963a, b):

$$KA = KA_0 / \sin(SE_{MD}) \quad (2\text{-}51)$$

where KA_0 is the KA for the vertical incident radiation (biome-specific value), and SE_{MD} is the solar elevation at midday (cf. Eq. 2-5). In Sim-CYCLE, LAI is a prognostic variable, given by the following:

$$LAI = SLA\, W_F / 2 \tag{2-52}$$

where SLA is the specific leaf area. Based on the assumption with respect to the light attenuation, we can substitute $PPFD_{IN}$ in Eq. 2-39 by Eq. 2-50, and integrate for the total leaf area index (LAI), in order to obtain the instantaneous rate GPP_{INS}:

$$\begin{aligned} GPP_{INS} &= \int_0^{LAI} PC\, dLAI \\ &= \frac{PC_{SAT}}{KA}\left[\ln\left\{QE + KA\, PPFD_{TOP}\right\} \right. \\ &\qquad \left. - \ln\left\{QE + KA\, PPFD_{TOP}\, \exp\left(-KA\, LAI\right)\right\}\right] \end{aligned} \tag{2-53}$$

According to Kuroiwa (1966), the diurnal change in $PPFD_{TOP}$ is well approximated by a square-sine curve with the peak at midday, in the following way (Fig. 2-20):

$$PPFD_{TOP} = PPFD_{MD} \sin^2\left(\frac{360 \cdot t}{DL}\right) \tag{2-54}$$

where t is the time from sunrise, DL is the day-length, and $PPFD_{MD}$ is the irradiance of $PPFD_{TOP}$ at midday. After substituting $PPFD_{TOP}$ by Eq. 2-54, we integrate Eq. 2-53 for DL to obtain the daily rate GPP_{DAY}:

$$GPP_{DAY} = \varepsilon \int_0^{DL} \int_0^{LAI} PC\, dLAI\, dt$$

$$= \frac{2\,\varepsilon\,PC_{SAT}DL}{KA}\left[\ln\left\{1+\sqrt{1+KA\cdot QE\cdot PPFD_{MD}/PC_{SAT}}\right\}\right.$$
$$\left.-\ln\left\{1+\sqrt{1+KA\cdot QE\cdot PPFD_{MD}\cdot\exp(-KA\cdot LAI)/PC_{SAT}}\right\}\right] \quad (2\text{-}55)$$

To translate the unit from μ mol CO_2 m^{-2} d^{-1} to Mg C ha^{-1} day^{-1}, the unit converter ε (=4.32 x 10^{-4}) and the monthly number of days are multiplied. Figure 2-21 shows that when *KA* is low, GPP_{DAY} increases linearly with increasing *LAI*, and that when *KA* is high, GPP_{DAY} saturates to *LAI*, suggesting that radiation use-efficiency depends strongly on the plant productive structure (Saeki, 1960).

2.2.4.2. Respiration

Although plant autotrophic plant respiration (*AR*) is one of the major CO_2 fluxes comparable to *GPP* and *NPP* in magnitude, our ability of modelling *AR* is insufficient, especially at the ecosystem scale. However, physiological studies (e.g., Hiroi and Monsi, 1964; McCree, 1970; Amthor, 1989) suggest that *AR* is composed of two components which have distinct functional meanings (i.e., for maintenance and for growth; Fig. 2-22), and that different plant organs respire at different rates. Then, we calculate *AR* as a sum of six processes:

$$AR = ARM + ARG$$
$$= \sum_{X=organ}^{F,C,R}(ARM_X) + \sum_{X=organ}^{F,C,R}(ARG_X) \quad (2\text{-}56)$$

where *ARM*s denote the maintenance respiration of whole plant, foliage, stem, and root, respectively, and similarly *ARG*s denote the growth respiration. The *ARM* is a function of the amount of standing carbon (*WP*) and temperature (*TG*) (Fig. 2-23):

$$ARM_X = SARM_X \exp\left[\frac{\ln(QT)}{10}(TG-15)\right] WP_X \quad (2\text{-}57)$$

where $SARM$ is the specific respiration rate, and TG is the temperature (control temperature, 15 °C). The term QT represents the sensitivity to temperature change. The typical value of QT is 2.0, ranging from 1.0 to 3.0 (Ryan, 1991), for various biomes and plant organs. However, as implied by Paembonan et al. (1992) and Yokota and Hagihara (1996), QT may acclimate seasonally in temperate and boreal ecosystems which experience a large temperature change between winter and summer. Based on their findings, QT is formulated as a function of temperature (Fig. 2-24):

$$QT = 2.0\exp\left[-0.009(TG-15)\right] \quad (2\text{-}58)$$

This modification results in a reduced sensitivity of ARM at higher temperatures, but we do not have sufficient data to characterize the biome-specificity. In forest ecosystems dominated by woody species, the maintenance respiration rate per unit biomass ($SARM$) for stem WP_C and root WP_R would decrease with accumulating passive woody tissues, or heartwood (Yokota et al., 1994; Yokota and Hagihara, 1998) (Fig. 2-25). The size-dependence of $SARM$s would be approximated by a function of standing biomass, given as (Fig. 2-26):

$$SARM = \phi_1 + \frac{\phi_2}{\phi_3 + \exp\left[\phi_4\left(WP - \phi_5\right)\right]} \quad (2\text{-}59)$$

where ϕ_1 to ϕ_5 are parameters. On the other hand, ARG is not an explicit function of environmental factors but a function of plant growth rate, because ARG represents the cost to produce new biomass (Amthor, 1989). Then, ARG is calculated only when biomass has net gain (i.e. $\Delta WP>0$), as follows:

$$ARG_X = SARG_X \, \Delta WP_X \cong SARG_X \frac{PT_X}{1 + SARG_X} \qquad (2\text{-}60)$$

where *SARG* is the specific growth respiration rate (foliage takes a higher value than stem and root), and *PT* is the photosynthate translocation to the organ (cf. Eq. 2-67). Consequently, *ARG* is indirectly regulated by environmental factors, via the rates of *GPP* and *ARM*. I note that *AR* does not directly respond to ambient CO_2 concentration, although several studies suggest that *AR* may be depressed by elevated CO_2 level (Wullschleger et al., 1994; Drake et al., 1997).

2.2.4.3. Decomposition

Soil organic carbon was divided into two compartments, because decomposition rate differs greatly between them. The labile part, litter WS_L, circulates once a few months or years, while the passive part, mineral soil WS_H, lingers for decades or centuries. Then, heterotrophic soil respiration *HR* is composed of two constituents from each compartment:

$$HR = HR_L + HR_H \qquad (2\text{-}61)$$

Both of HR_L and HR_H are affected by temperature and soil moisture conditions:

$$HR_L = SHR_L \cdot WS_L \cdot F_{HRL}(TS_{10}) \cdot F_{HRL}(MS_{UP}) \qquad (2\text{-}62a)$$

$$HR_H = SHR_H \cdot WS_H \cdot F_{HRH}(TS_{200}) \cdot F_{HRH}(MS_{LW}) \qquad (2\text{-}62b)$$

where SHR_L and SHR_H are the specific respiration rates, respectively, and $F_{HRL}()$s and $F_{HRH}()$s are the coefficient functions of temperature and soil moisture conditions, respectively. For the temperature dependence, the exponential function similar to one in Eq. 2-57 has been frequently used, but Lloyd and Taylor (1994) showed that the exponential function is not the best model, and they alternatively proposed an Arrhenius-type model (Fig. 2-27):

$$F_{HR}(TS) = \exp\left[308.56\left(\frac{1}{56.02} - \frac{1}{TS + 46.02}\right)\right] \quad (2\text{-}63)$$

where TS is the soil temperature (TS=TS_{10} for WS_L, and TS=TS_{200} for WS_H). Equation 2-63 leads to lower responsiveness at higher temperatures than the exponential one (Lloyd and Taylor, 1994; Kirschbaum, 1995, 2000). Although we do not explicitly include the effect of soil freezing, this would have a negligible effect on the HR estimation. The coefficient function with respect to soil moisture $F_{HR}(MS)$ is the minimum of two contrasting components (Fig. 2-28):

$$F_{HR}(MS) = \min\{F_{HR}(WA), F_{HR}(AE)\} \quad (2\text{-}64)$$

The term $F_{HR}(WA)$ represents the effect of soil moisture on microbial activity, while the term $F_{HR}(AE)$ represents the effect of soil air space (i.e. anaerobic condition):

$$F_{HR}(WA) = WA_0 + \frac{MS/WHC}{KM_{WA} + MS/WHC} \quad (2\text{-}65a)$$

$$F_{HR}(AE) = AE_0 + \frac{(1 - MS/WHC)}{KM_{AE} + (1 - MS/WHC)} \quad (2\text{-}65b)$$

where WA_0 and AE_0 are the minimum values, KM_{WA} and KM_{AE} are the parameters related to responsiveness, and WHC is the water holding capacity. In sum, a larger MS increases HR under dry conditions, whereas a larger MS reduces HR near water saturation (Fig. 2-28).

2.2.4.4. Litterfall

At the equilibrium state, the amount of annual LF must be identical to that of annual NPP, so that plant biomass becomes stable. However, the shedding of dead biomass is one of

the most difficult processes for mechanistic models, and then a constant mortality or turnover rate irrespective of environmental conditions is assumed for evergreen biomes:

$$LF = \sum_{X=organ}^{F,C,R} \left(SLF_X \; WP_X \right) \tag{2-66}$$

where SLF is the specific litter fall rate, or mortality. In grasslands, plants shed most of their shoots (WP_F and WP_C) during winter (C_3, $TG<5°C$; C_4, $TG<8°C$) or dry season ($MS<0.1WHC$), while their root has a constant mortality (Pearcy and Ehleringer, 1984). Figure 2-29 illustrates the phenological cycle in temperate and boreal deciduous forests, using two thermal indices: mean air temperature and cumulative temperature above 5°C from the beginning of the year. Dormancy is broken when cumulative temperature exceeds 200°C•days, while leaves are shed when mean temperature falls below 5°C (Reich et al., 1992).

2.2.4.5. Photosynthate translocation

Although modelling of photosynthate allocation PT is far from sufficient to be mechanistic (Cannell and Dewar, 1994), the dry-matter production theory would present keys to address it. At first, Monsi (1960) made the schematic diagram of plant growth, from CO_2 assimilation to biomass increment (Fig. 2-30). This scheme suggests that assimilated carbon should be partitioned among plant organs, after subtracting the maintenance cost of plant organs(ARM):

$$EP = GPP - ARM = \sum_{X=organ}^{F,C,R} \left(PT_X \right) \tag{2-67}$$

where EP is the effective photosynthate to growth. If the EP is negative, translocation and vegetative growth can not be expected. Accordingly, the positive EP would be partitioned among WP_F, WP_C, and WP_R, such that the fixed carbon is utilized by plants most profitably to

survive. At second, Kuroiwa (1966) derived the optimal leaf area index (LAI_{OPT}), which can maximize the daily net carbon uptake, from the daily *GPP* estimation by Eq. 2-55, in the following way:

$$LAI_{OPT} = \frac{1}{KA}\ln\left[\frac{KA \cdot QE \cdot PPFD_{MD}}{PC_{SAT}\left\{PC_{SAT} \cdot DL/\left(PC_{SAT} - DCST\right) - 1\right\}}\right] \tag{2-68}$$

where *DCST* is the daily cost to maintain the unit amount of foliage:

$$DCST = \frac{\left[SARM_F + SLF_F\left(1 + SARG_F\right)\right]}{2\ SLA} \tag{2-69}$$

When the community *LAI* is identical to the LAI_{OPT}, almost all leaves, even ones at the bottom of canopy, may perform as a carbon source; in other words, this model prohibits heterotrophic leaves (i.e. performing as a carbon sink) to exist. Many empirical studies support the shoot independence in terms of carbon economy, and then the theoretical prediction of LAI_{OPT} will be a valid indicator of carbon allocation to WP_F. Thus, if *EP* is positive, photosynthate is firstly allocated to WP_F, so that it becomes close to LAI_{OPT}. It is notable that an excessive amount of carbon should not be allocated to WP_F to avoid overshooting, and that the LAI_{OPT} can be enlarged by stimulating the photosynthetic capacity, i.e. *QE* and PC_{SAT}. The residual carbon is allocated to WP_C and WP_R with a constant ratio, in order to realize the biome-specific growth-form; woody biomes invest a considerable fraction to stem WP_C, while herbaceous biomes mostly to root WP_R.

2.2.4.6. C_3-C_4 mixed community

The ecosystem-scale productivity and biomass in a C_3-C_4 mixed grassland is, for example, calculated as follows (Fig. 2-31):

$$NPP = F_{C3} \cdot NPP_{C3} + F_{C4} \cdot NPP_{C4} \quad (2\text{-}70)$$

where F_{C3} and F_{C4} are the fractional ground coverage by C_3 and C_4 species ($F_{C3}+F_{C4}=1$), respectively, and NPP_{C3} and NPP_{C4} are the productivity of C_3 and C_4 plants per unit area coverage. However, net radiation *RNC* and transpiration *TR* are calculated only at the plot-scale, assuming the canopy as a single big-leaf. In simulation practices, F_{C3} and F_{C4} are derived from field data (i.e. plot-scale) or estimated based on an empirical relationship (Ehleringer et al., 1997; Collatz et al., 1998).

2.2.4.7. Efficiency of dry-matter production

Two parameters show how efficient plants produce dry matter using a finite quantity of resources: water use efficiency *WUE* and radiation use efficiency *RUE* (Jones, 1992). *WUE* indicates the amount of assimilated carbon per unit transpired water from the canopy:

$$WUE = NPP / TR \quad (2\text{-}71)$$

On the other hand, *RUE* indicates the amount of assimilated carbon per unit absorbed PAR by the canopy (cf. Eq. 2-14):

$$RUE = NPP / PAR_{ABS} \quad (2\text{-}72)$$

$$APAR = 7.1 \cdot PPFD_{TOP} IR \quad (2\text{-}73)$$

where a constant of 7.1 converts unit into MJ m^{-2} yr^{-1}. These efficiencies were calculated both for each month and for annual total.

Table 2-1. Ecophysiological differences between C_3 and C_4 plants in Sim-CYCLE.

Physiological component	C_3 plants	C_4 plants
quantum yield (QE)	a function of surface temperature and intercellular CO_2 concentration (0.03~0.07 mol CO_2 mol^{-1} photon)	a constant (0.05 mol CO_2 mol^{-1} photon)
light-saturated photosynthesis (PC_{SAT})	lower (5~20 μ mol CO_2 m^{-2} s^{-1})	higher (15~30 μ mol CO_2 m^{-2} s^{-1})
stomatal conductance GS	slightly higher (200-450 mmol H_2O m^{-2} s^{-1})	slightly lower (150-400 mmol H_2O m^{-2} s^{-1})
CO_2 compensation point (CD_{CMP})	higher, and a function of surface temperature (30~50 ppmv)	lower, and a constant (5 ppmv)
optimum temperature of photosynthesis (T_{OPT})	lower, and a function of intercellular CO_2 concentration (15~25 ℃)	higher, and a constant (25~30 ℃)
minimum temperature of photosynthesis (T_{MIN})	lower (-3~5 ℃)	higher (8 ℃)
CO_2 dependence parameter (KM_{CD})	higher (30~80 ppmv)	lower (5~10 ppmv)

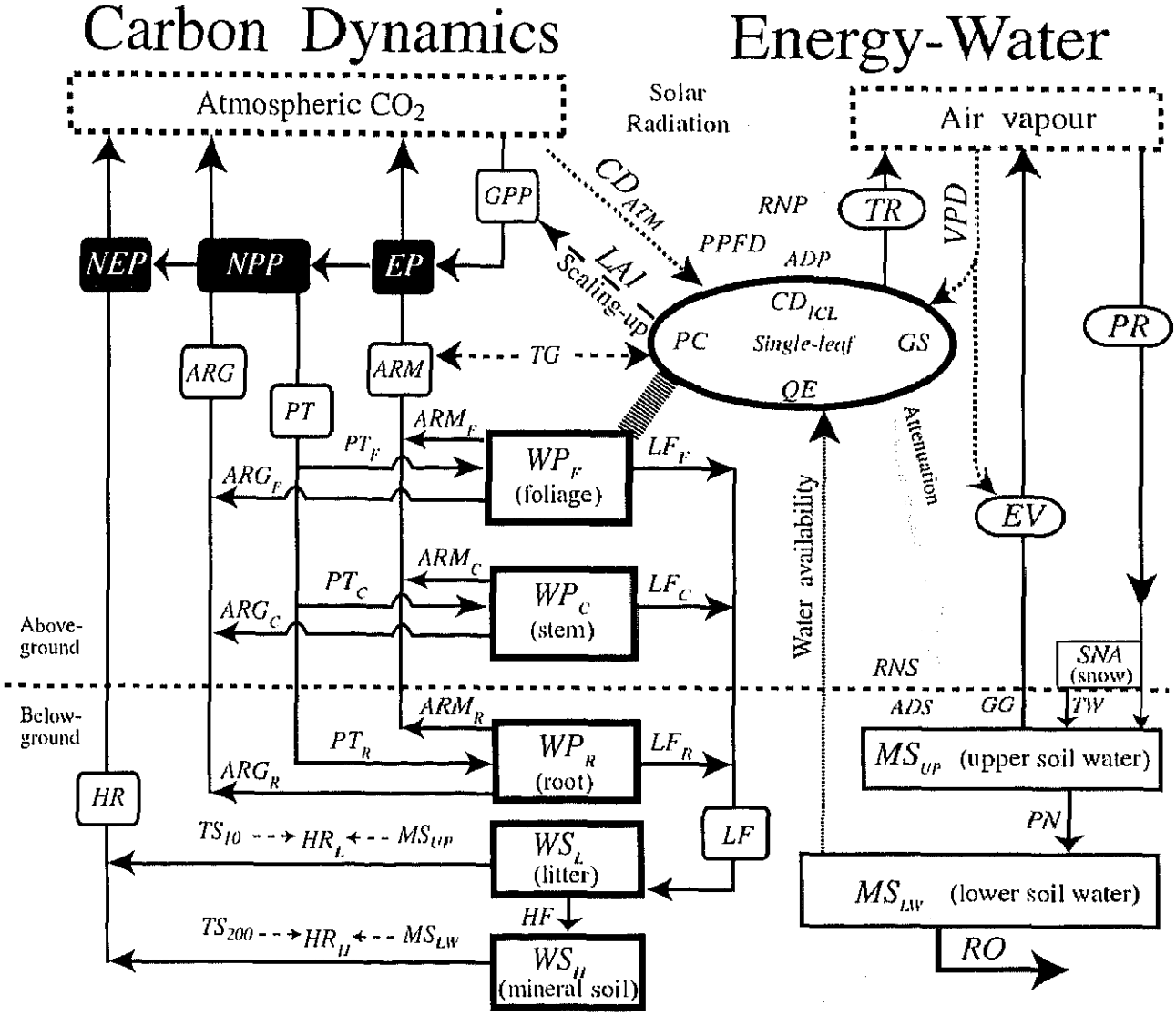

Fig. 2-1. Schematic diagram of Sim-CYCLE. The carbon storage of a terrestrial ecosystem is divided into five compartments, in the middle of the picture: WP_F (foliage), WP_C (stem and branch), WP_R (root), WS_L (litter, or dead biomass), and WS_H (mineral soil). Leftward; carbon fluxes among the compartments are arranged, including gross primary production *GPP*, maintenance respiration *ARM*, translocation *PT*, growth respiration *ARG*, litterfall *LF*, and soil heterotrophic respiration *HR*. The terms *EP*, *NPP*, and *NEP* denote effective photosynthate for growth (=*GPP-ARM*), net primary production (=*EP-ARG*), and net ecosystem production (=*NPP-HR*), respectively. In a single-leaf (depicted by an oval), stomatal conductance *GS*, intercellular CO_2 concentration CD_{ICL}, light use efficiency *QE*, and photosynthetic carbon assimilation *PC* are determined interactively, as functions of such various environmental factors as photosynthetic photon flux density *PPFD*, atmospheric CO_2 concentration CD_{ATM}, surface temperature *TG*, soil water availability *MS*s, and ambient vapor pressure deficit *VPD*. Rightward; water and energy budget in the ecosystem is given. The precipitation (*PR*) is divided into soil water storage (*MS*), evaporation from soil surface (*EV*) and canopy surface (*IC*), transpiration from the canopy (*TR*), and subsurface runoff (*RO*). The *TR* and *EV* depend respectively on the energy inputs on canopy (*RNP*) and soil (*RNS*), which are affected by surface albedo (*ADP* and *ADS*).

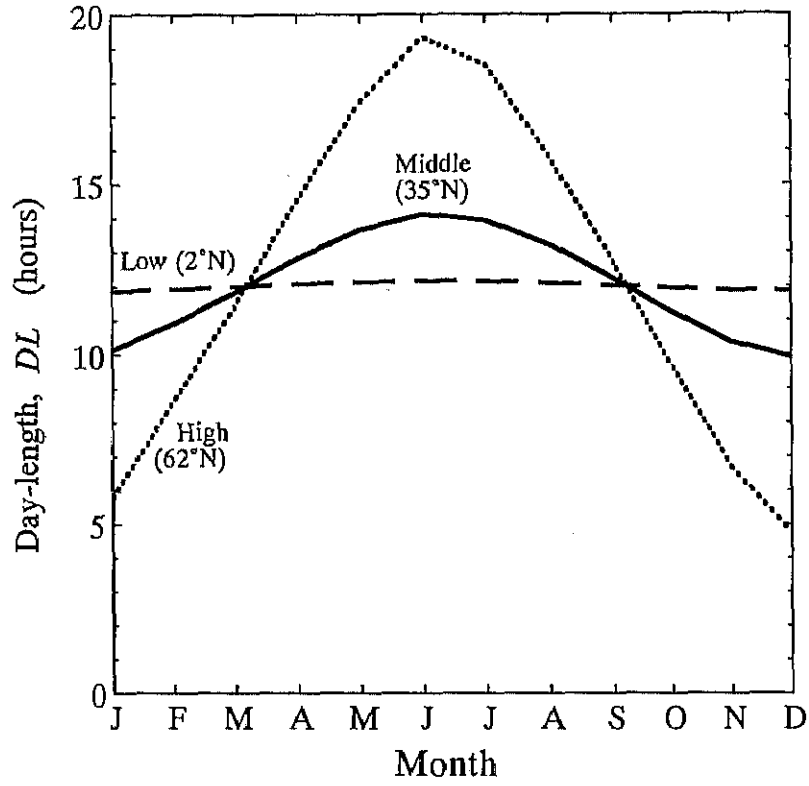

Fig. 2-2. Seasonal change in day-length DL.

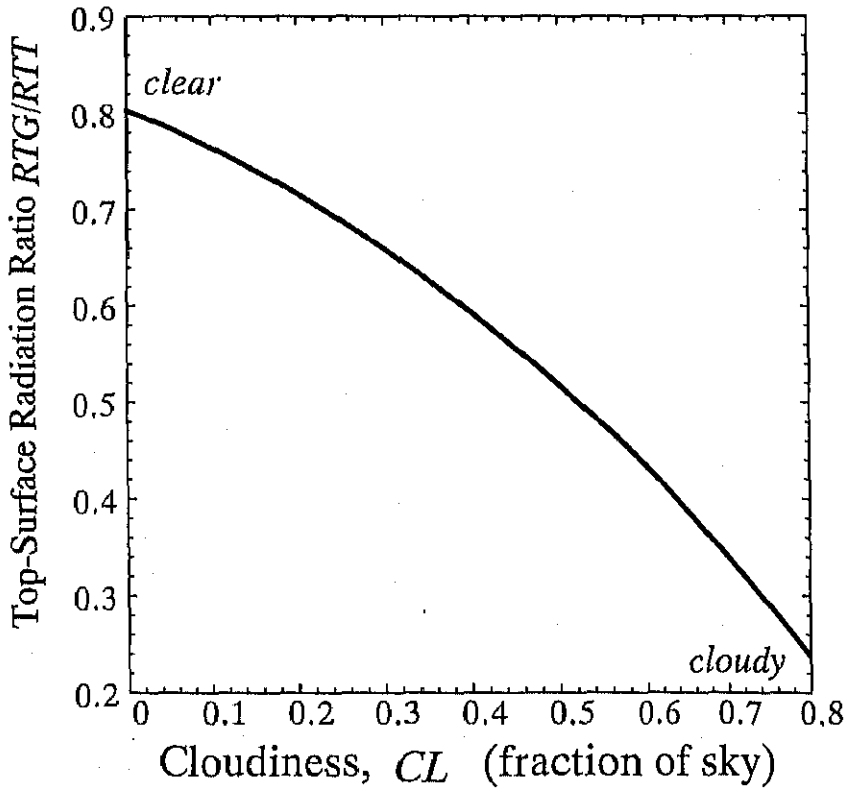

Fig. 2-3. Relationship between cloudiness and surface radiation.

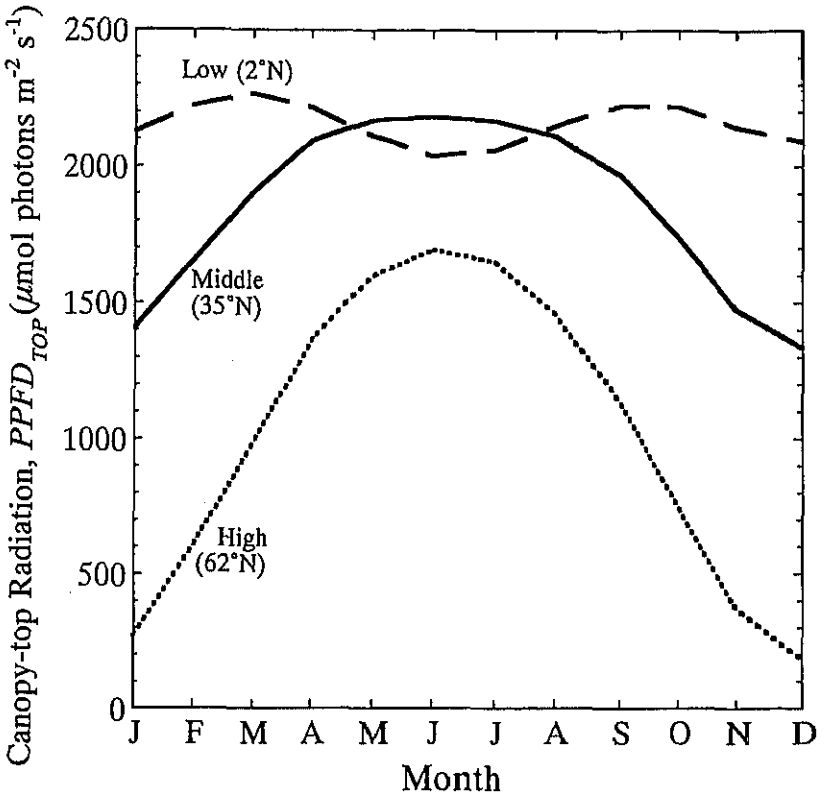

Fig. 2-4. Seasonal change in canopy-top photosynthetic photon flux density (clear sky).

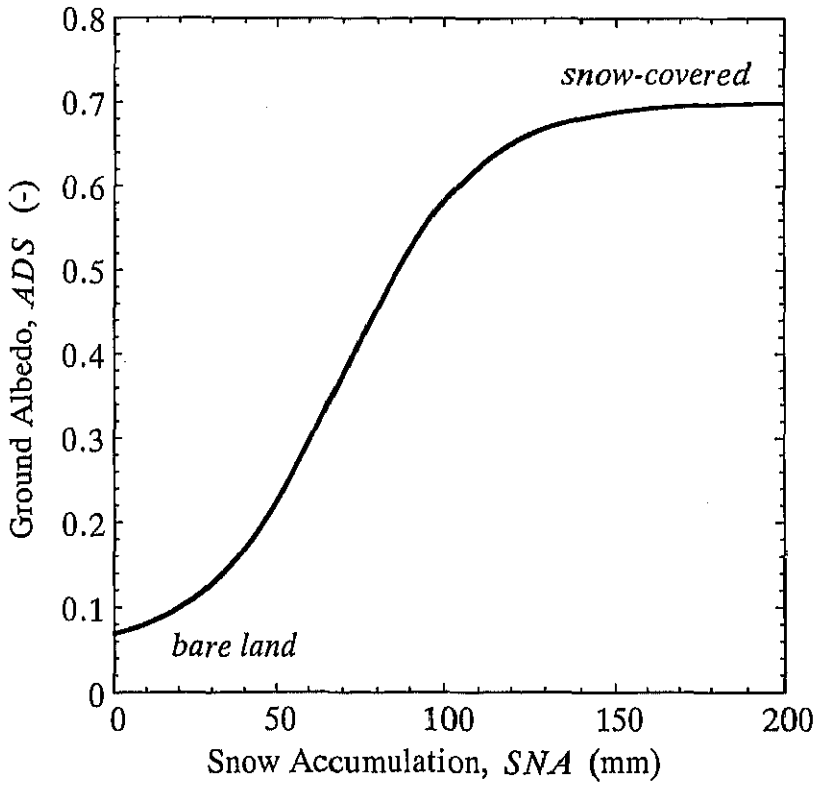

Fig. 2-5. Relationship between snow accumulation and surface albedo.

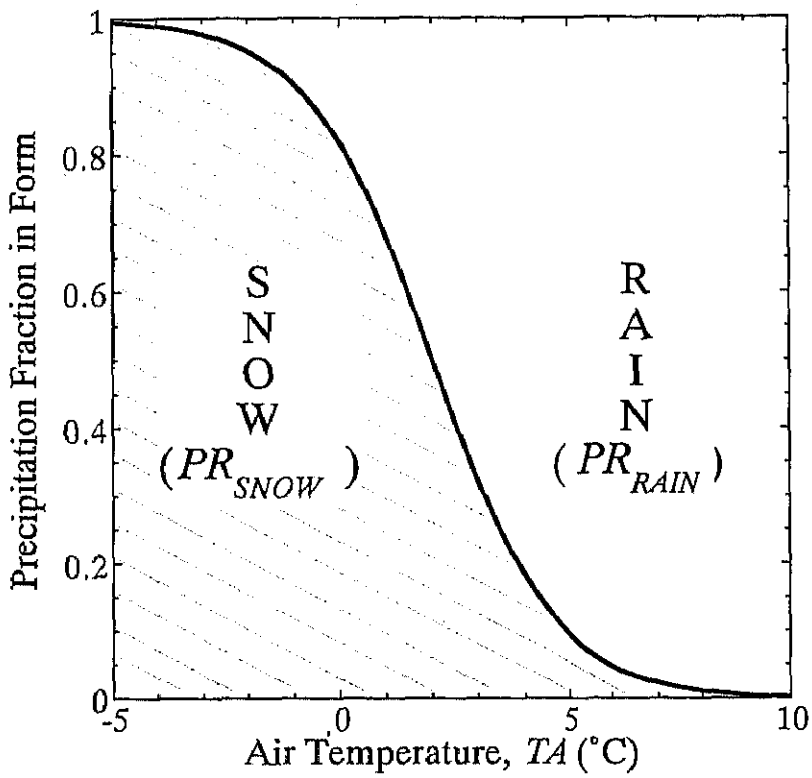

Fig. 2-6. Fractional change between snow and rain precipitation with increasing air temperature.

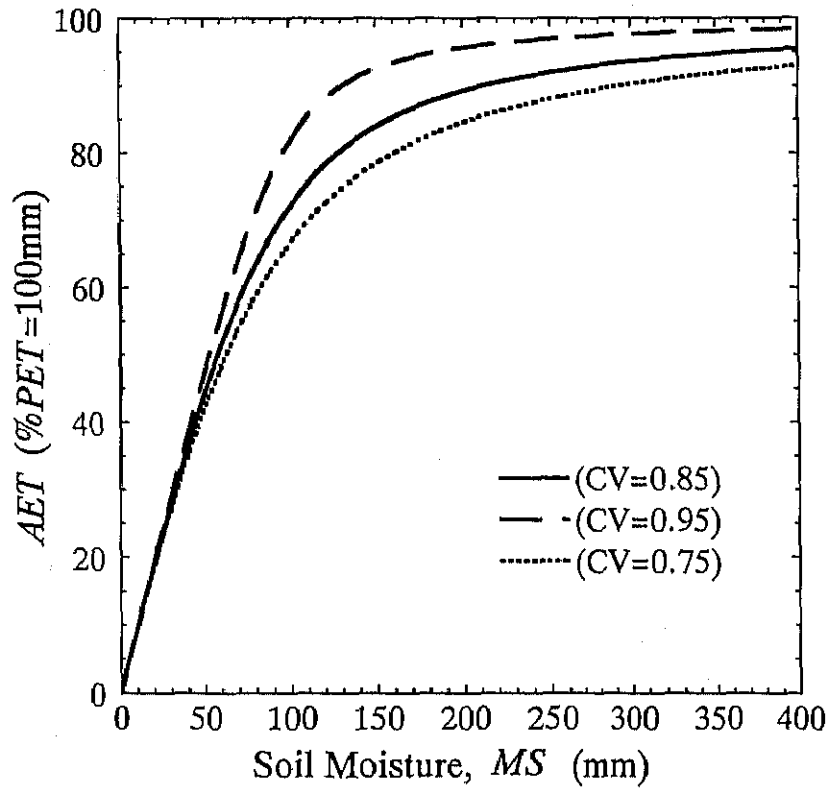

Fig. 2-7. Relationship between soil moisture content and actual evapotranspiration.

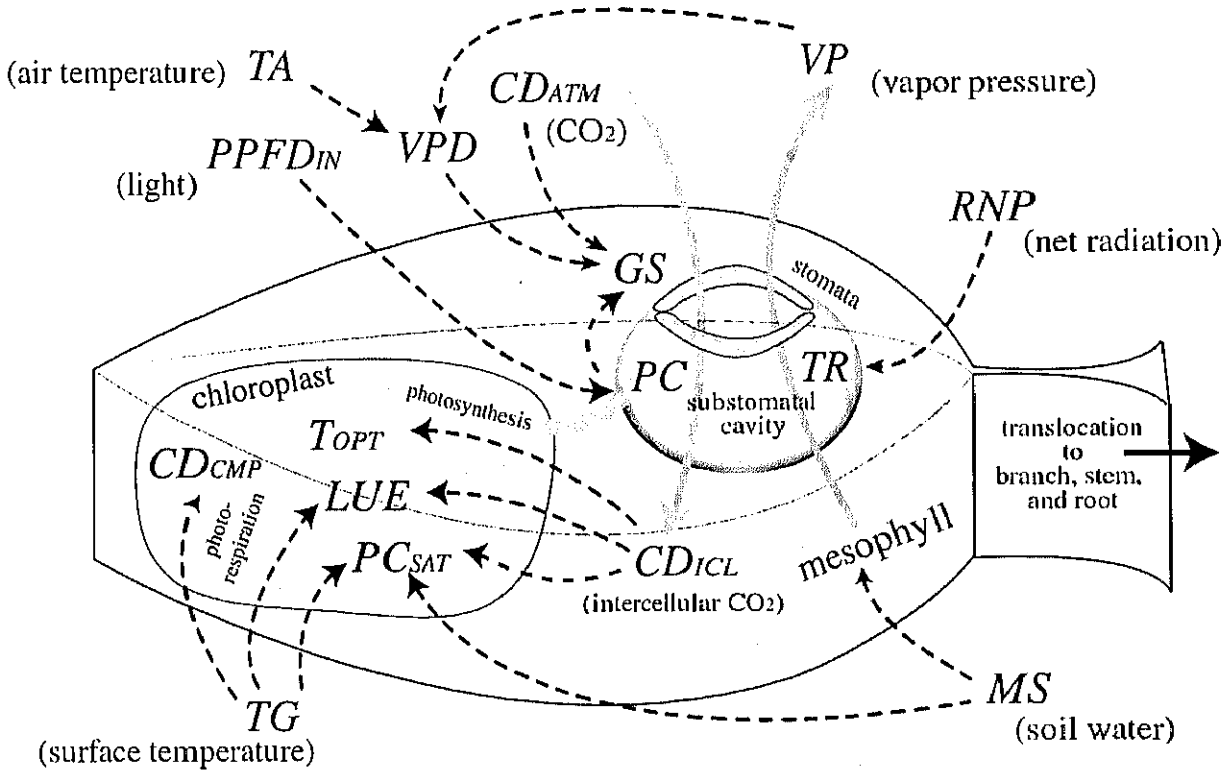

Fig. 2-8. Schematic diagram of single-leaf processes. CO_2 and H_2O(vapor) are exchanged through stomata, i.e. photosynthesis *PC* and transpiration *TR*, respectively. The conductance of stomata *GS* is regulated by atmospheric CO_2 concentration CD_{ATM}, vapor pressure deficit *VPD*, and photosynthetic rate *PC*. The term *PC* is a function of irradiance of photosynthetically active radiation $PPFD_{IN}$, intercellular CO_2 concentration CD_{ICL}, surface temperature TG, and soil moisture content *MS*. In the calculation, photosynthetic properties, i.e. light use efficiency *LUE*, CO_2 compensation point CD_{CMP}, and optimum temperature T_{OPT}, are also estimated. The term *TR* is affected by net radiation *RNP* and *VPD* (a function of air vapor pressure*VP* and air temperature *TA*).

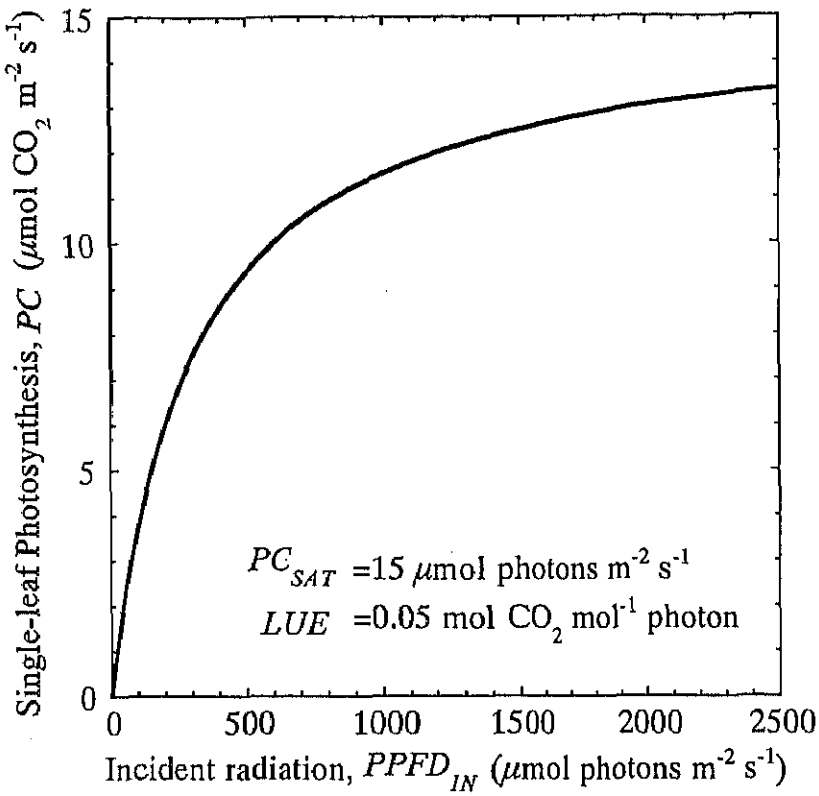

Fig. 2-9. Relationship between irradiance and single-leaf photosynthetic rate.

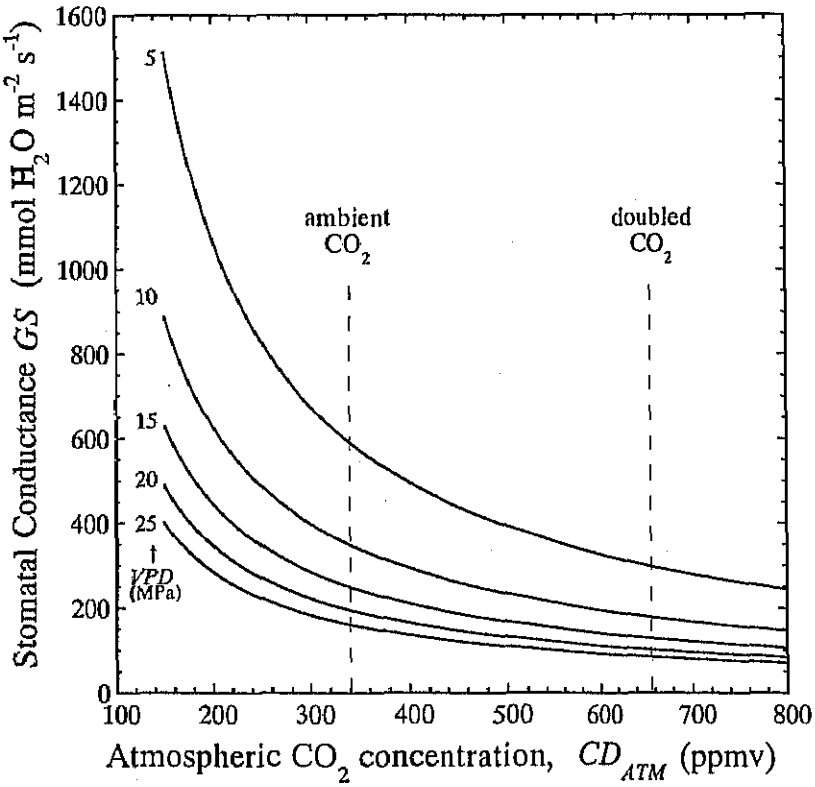

Fig. 2-10. Relationship between atmospheric CO_2 concentration and stomatal conductance, for different *VPD* s.

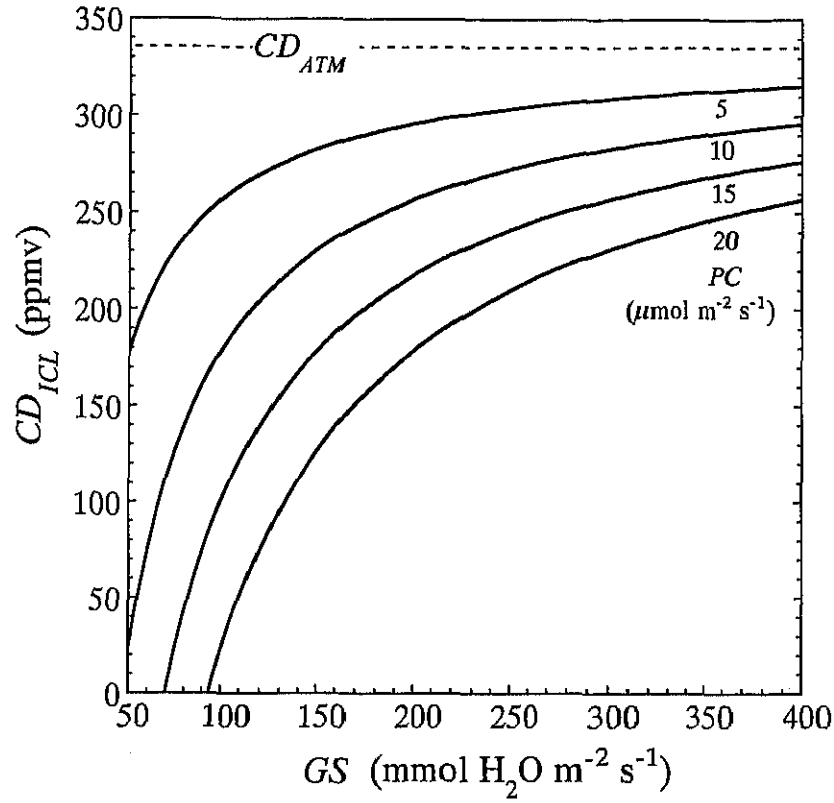

Fig. 2-11. Relationship between stomatal conductance and intercellular CO_2 concentration, for different *PC* s.

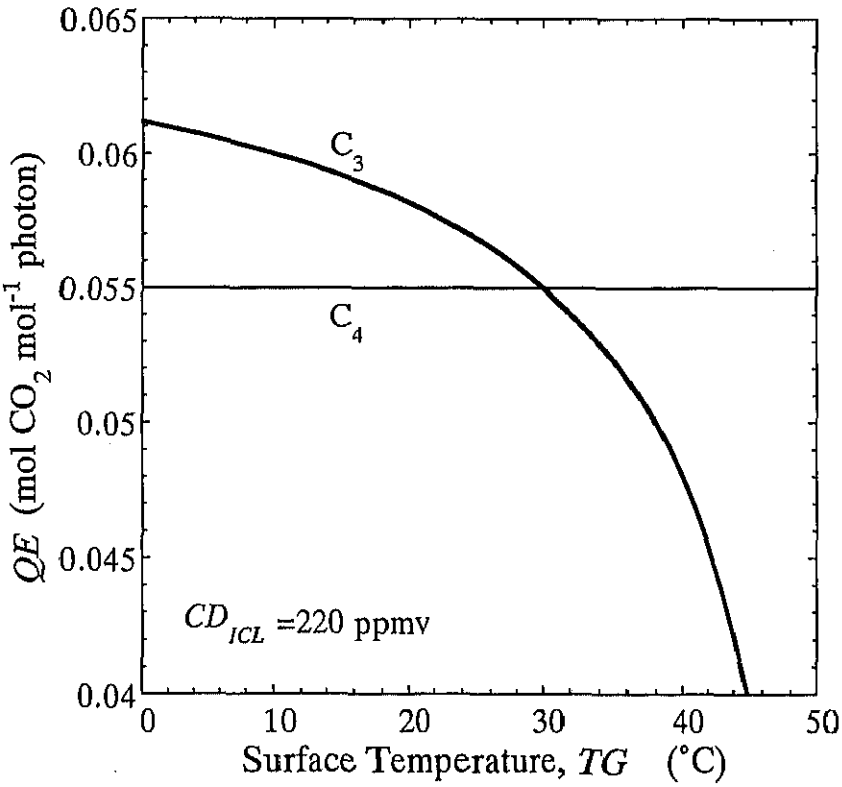

Fig. 2-12. Relationship between temperature and photosynthetic light-use efficiency.

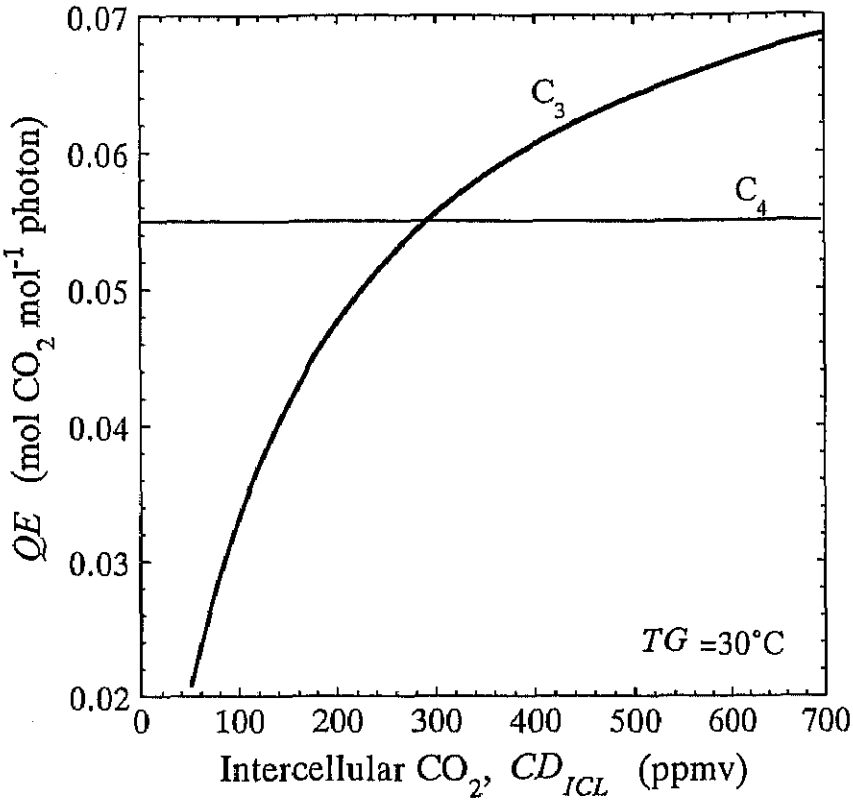

Fig. 2-13. Relationship between intercellular CO_2 concentration and photosynthetic light-use efficiency.

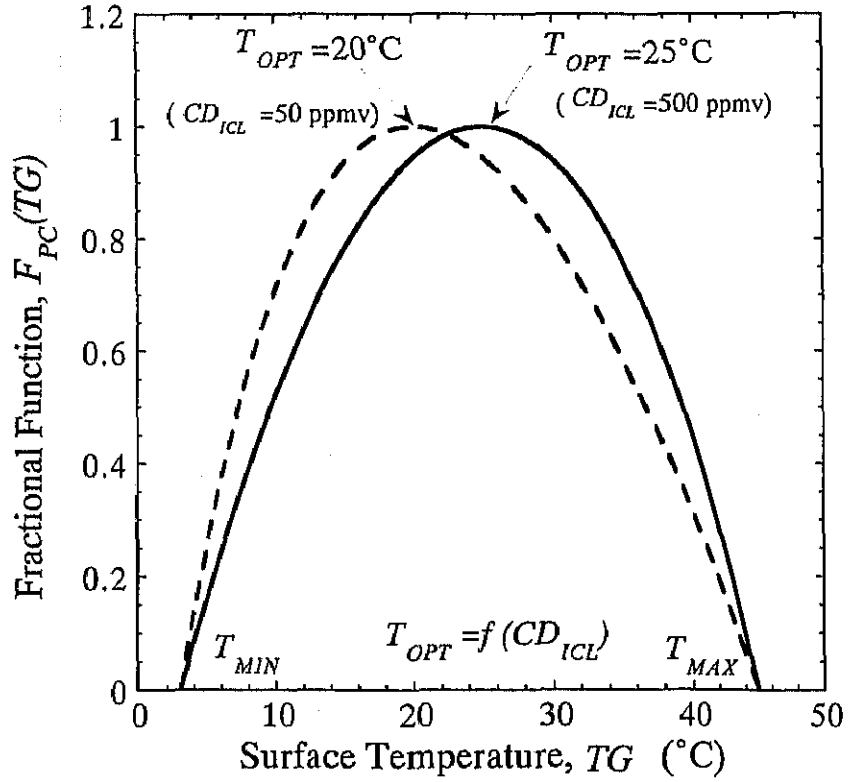

Fig. 2-14. Relationship between temperature and photosynthetic capacity.

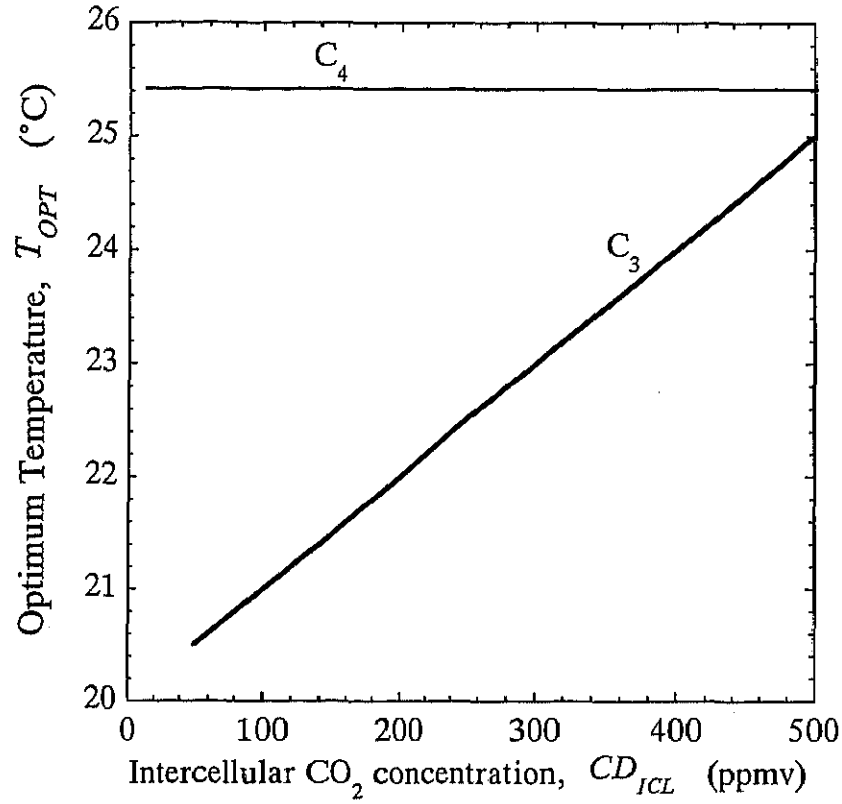

Fig. 2-15. Relationship between intercellular CO_2 concentration and optimum temperature for photosynthesis.

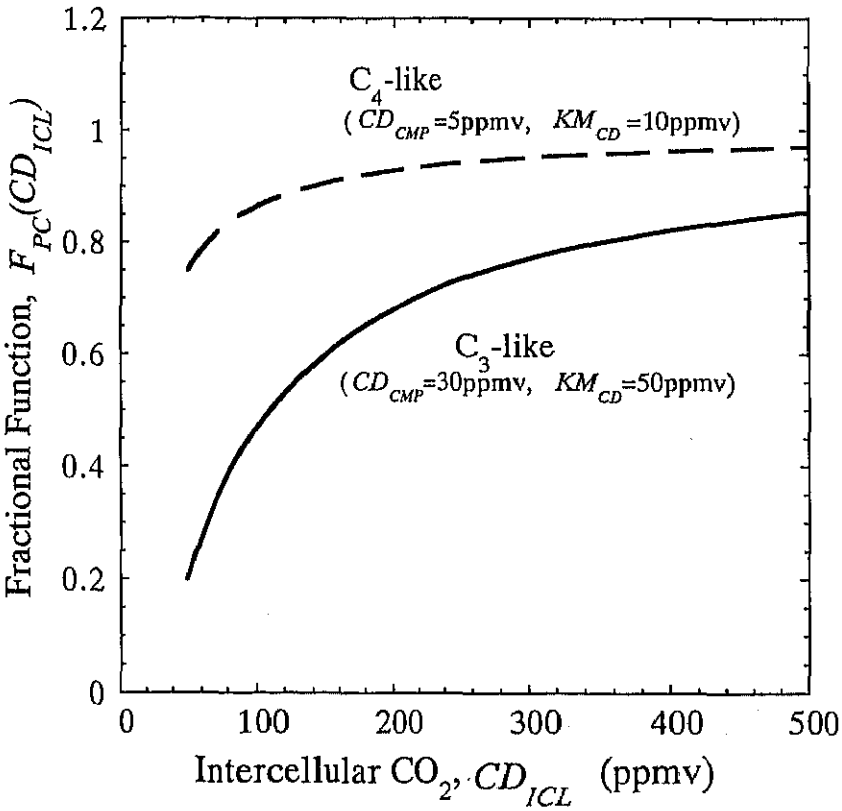

Fig. 2-16. Relationship between intercellular CO_2 concentration and single-leaf photosynthetic rate.

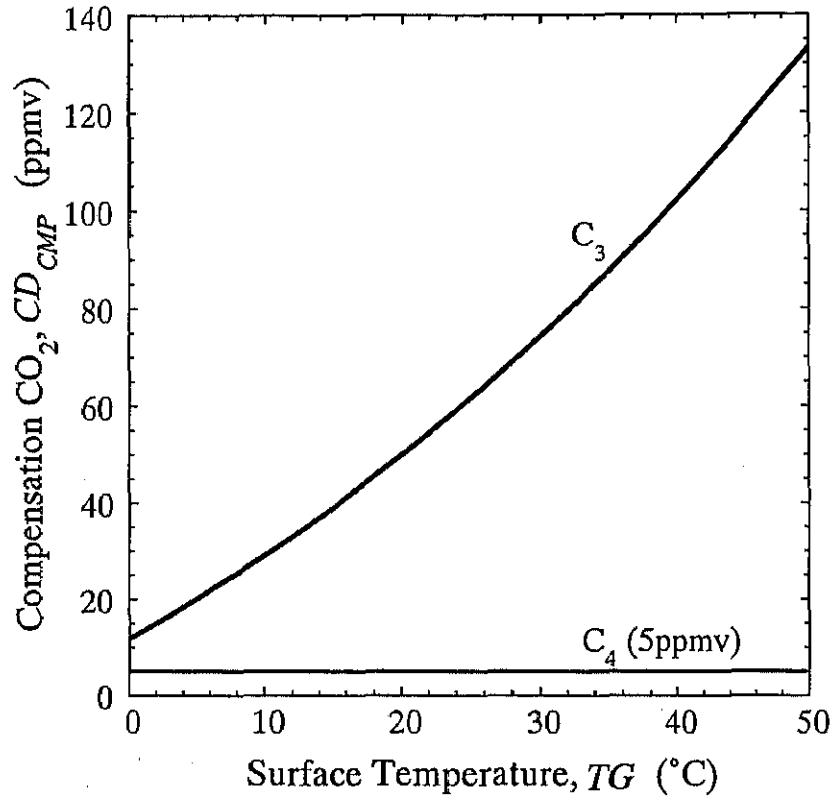

Fig. 2-17. Relationship between temperature and photosynthetic CO_2 compensation point.

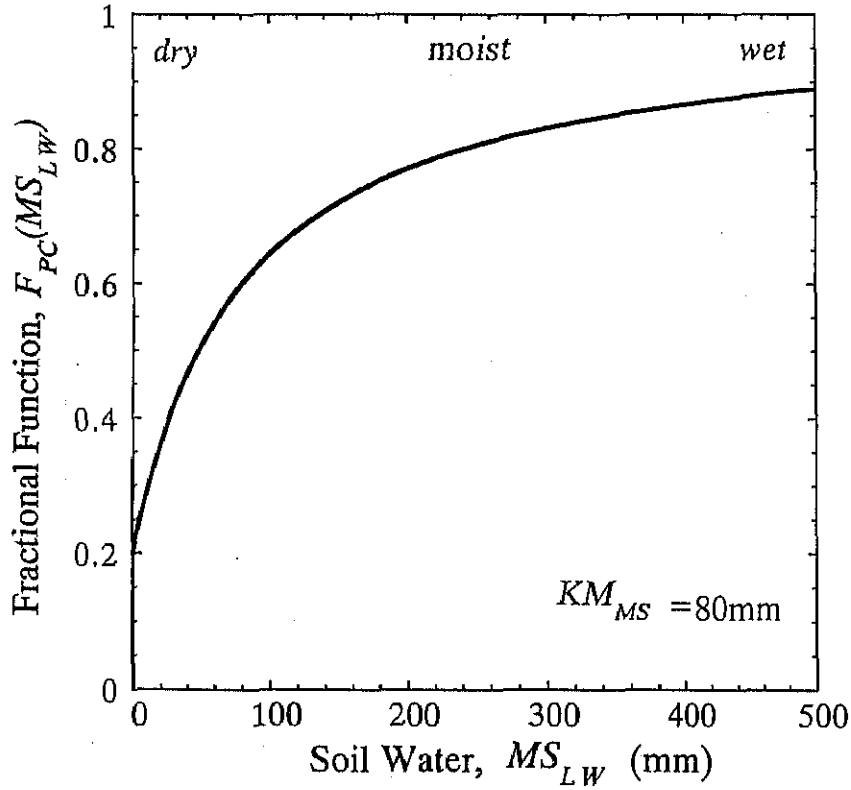

Fig. 2-18. Relationship between soil moisture content and photosynthetic capacity.

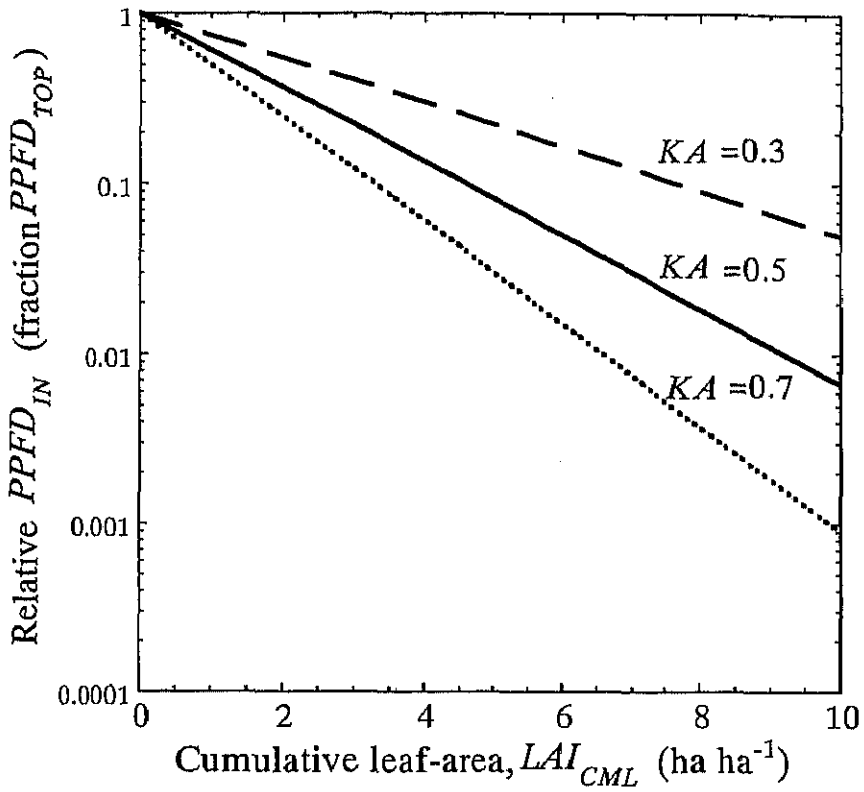

Fig. 2-19. Relationship between cumulative leaf area index and relative irradiance of PAR.

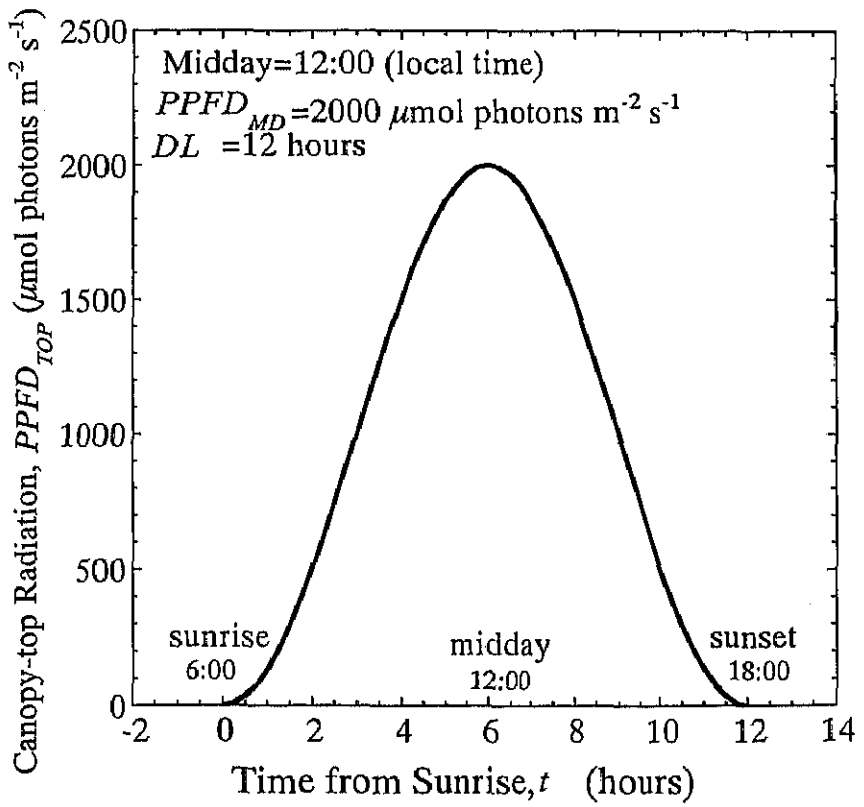

Fig. 2-20. Diurnal change in canopy-top PAR (clear day).

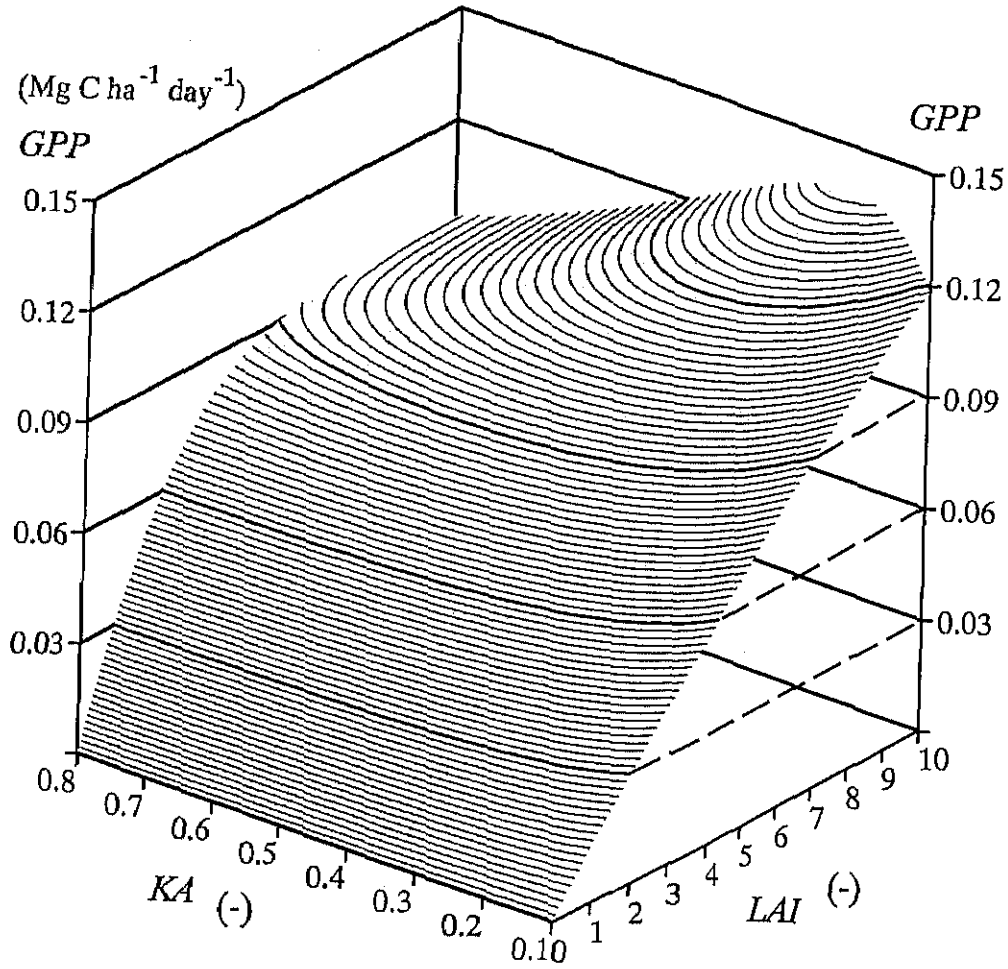

Fig. 2-21. Relationship between *GPP* and canopy properties, i.e. leaf area index *LAI* and attenuation coefficient *KA*.

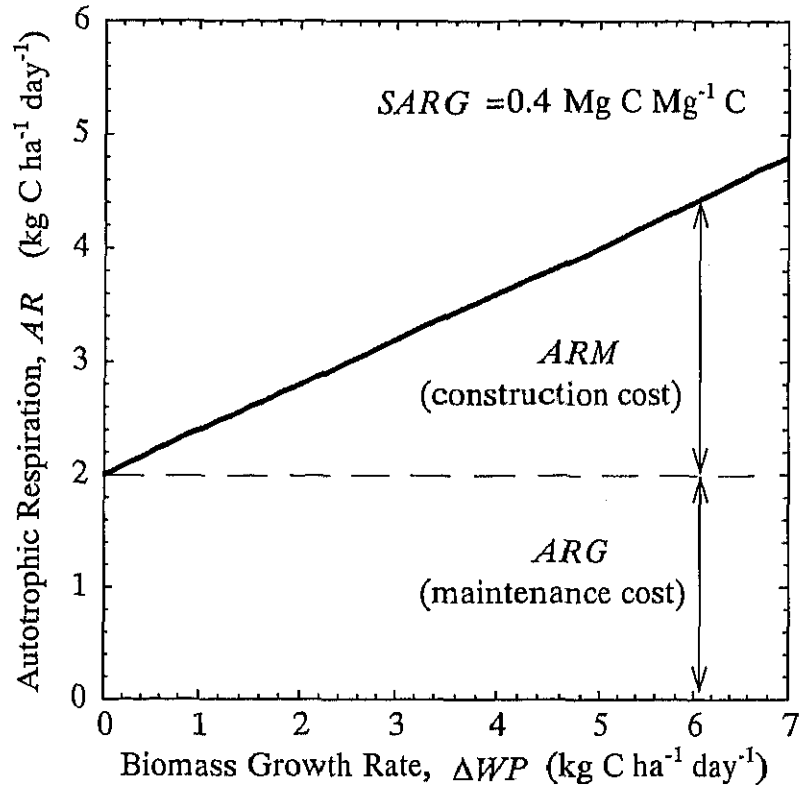

Fig. 2-22. Relationship between growth rate and respiration rate, which is composed of maintenance and growth components.

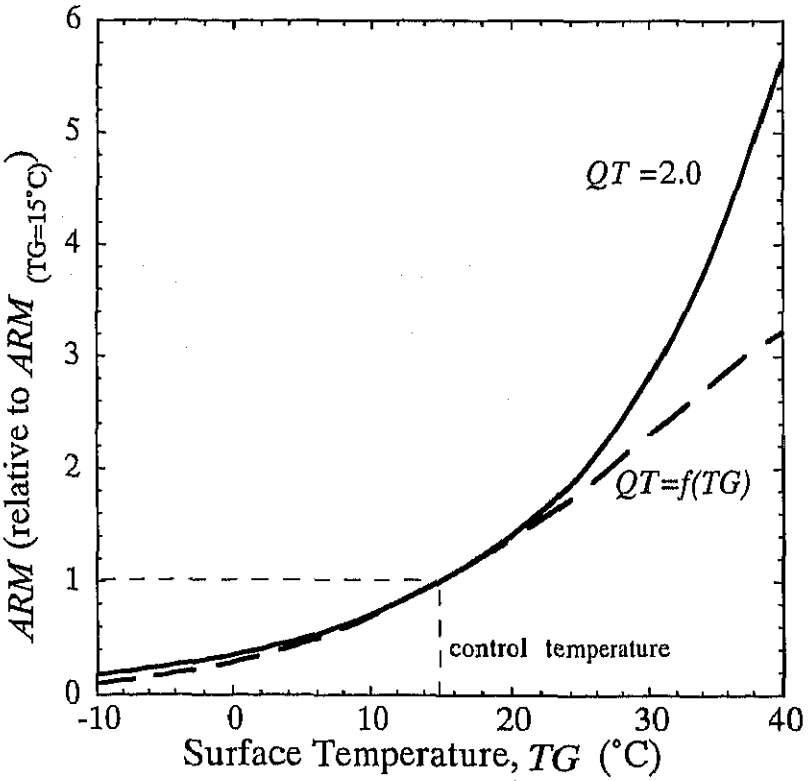

Fig. 2-23. Relationship between temperature and maintenance respiration rate.

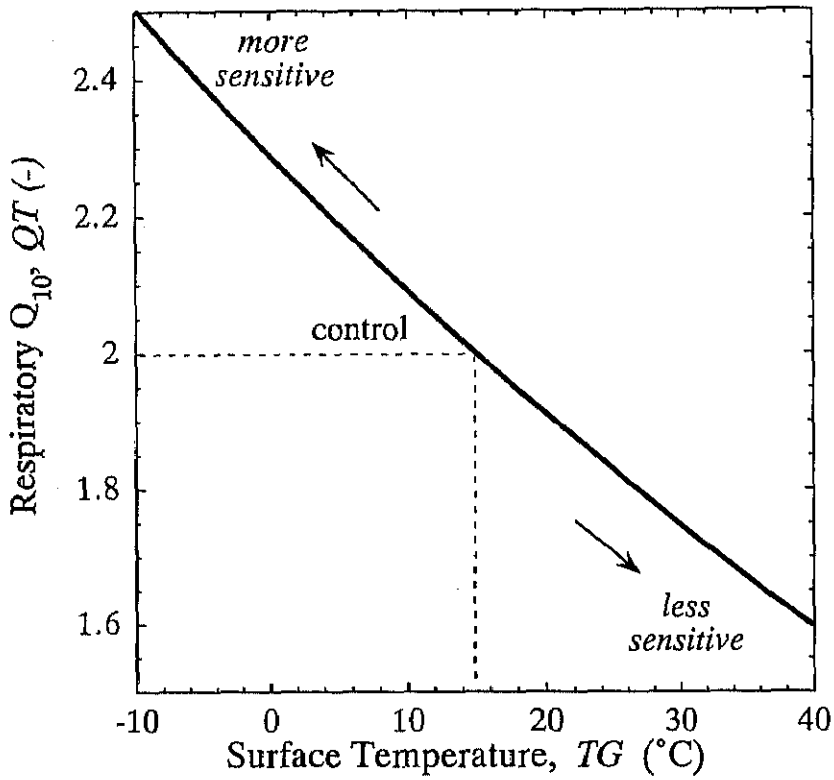

Fig. 2-24. Relationship between temperature and respiratory temperature dependence Q_{10}.

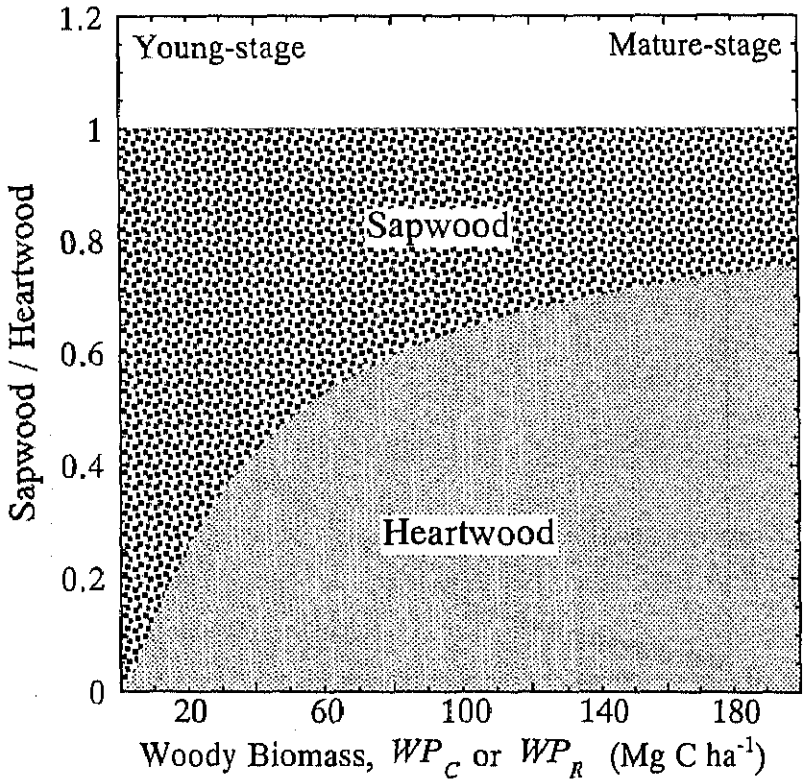

Fig. 2-25. Relationship between woody biomass and fraction of sapwood and heartwood.

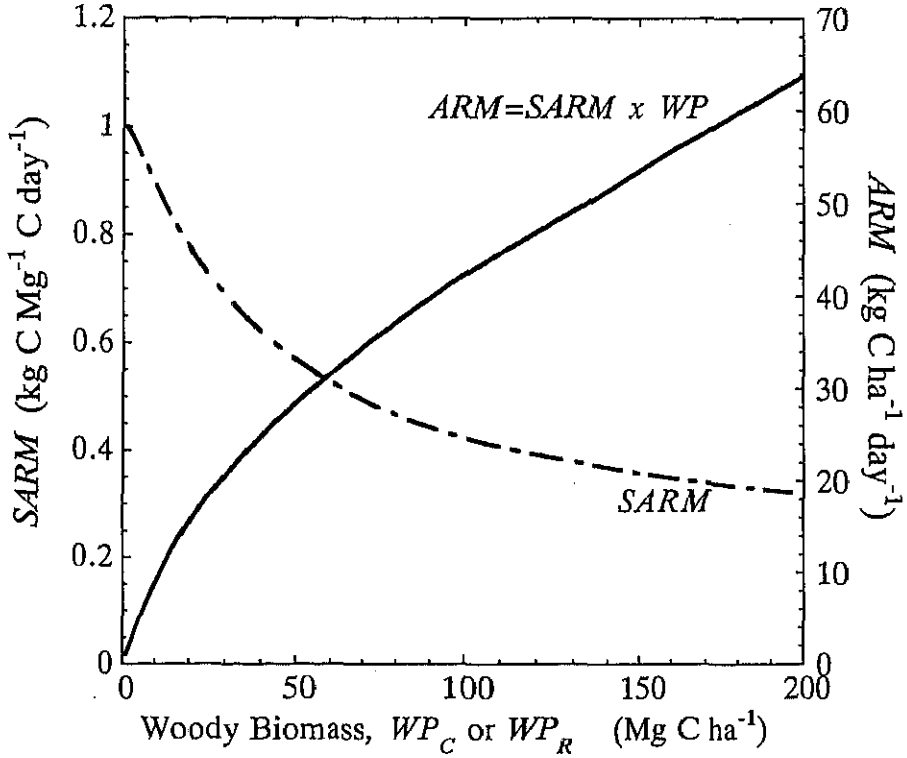

Fig. 2-26. Relationship between woody biomass of stem and root compartments and specific and total respiration rates.

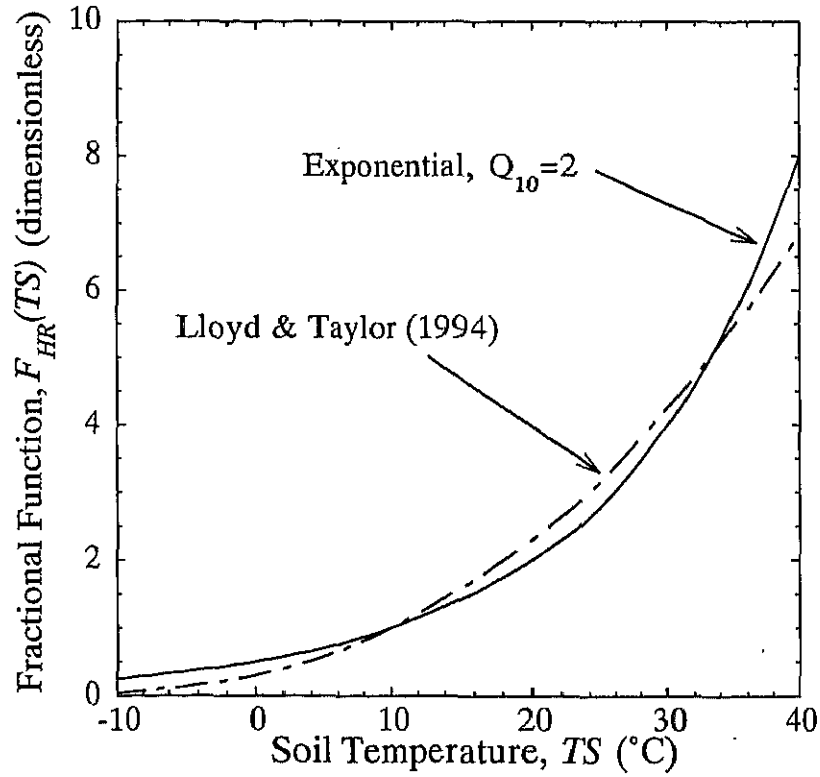

Fig. 2-27. Relationship between soil temperature and soil decomposition rate.

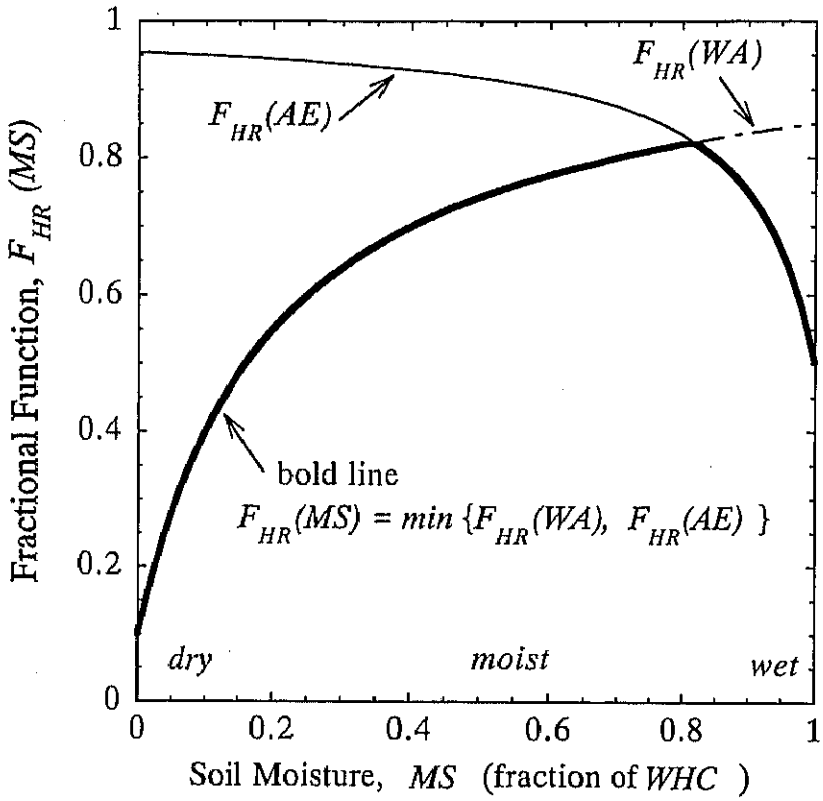

Fig. 2-28. Relationship between soil moisture content and soil decomposition rate, regulated by water and air availabilities.

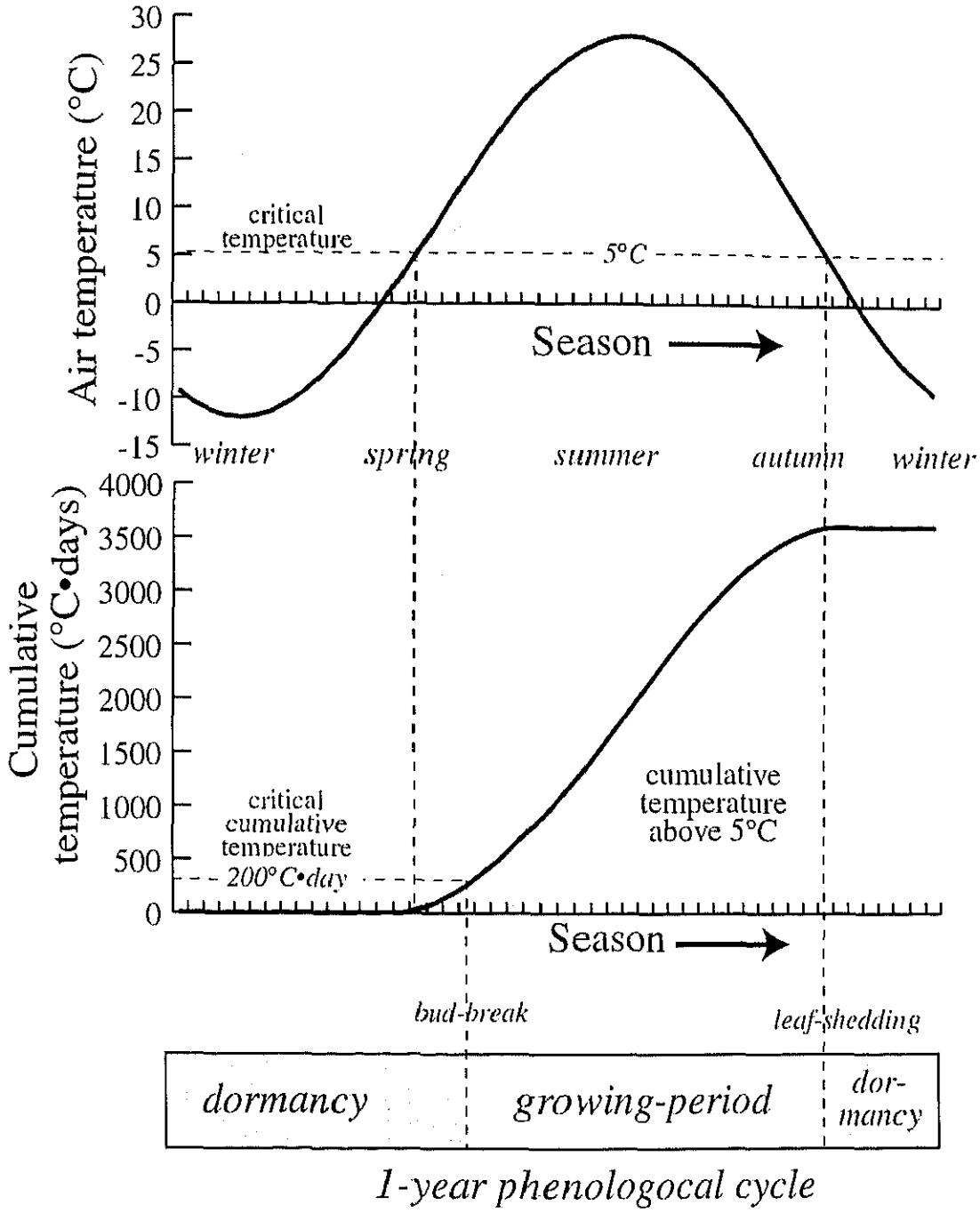

Fig. 2-29. Phenological cycle of temperate deciduous biomes from dormancy breaking in spring to leaf shedding in autumn, based on two thermal indices, i.e. air temperature and cumulative temperature.

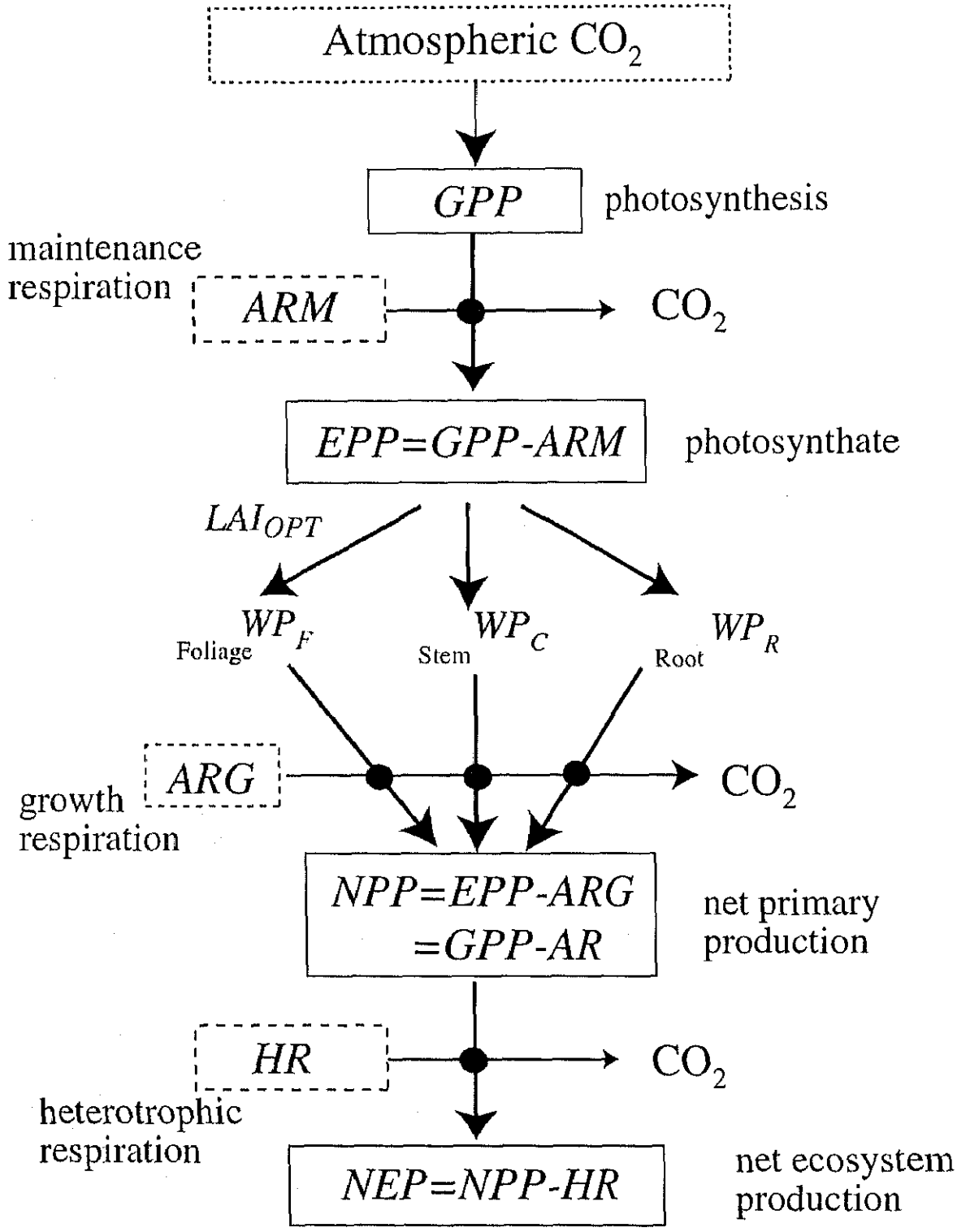

Fig. 2-30. Schematic disgram of the production scheme of Sim-CYCLE.

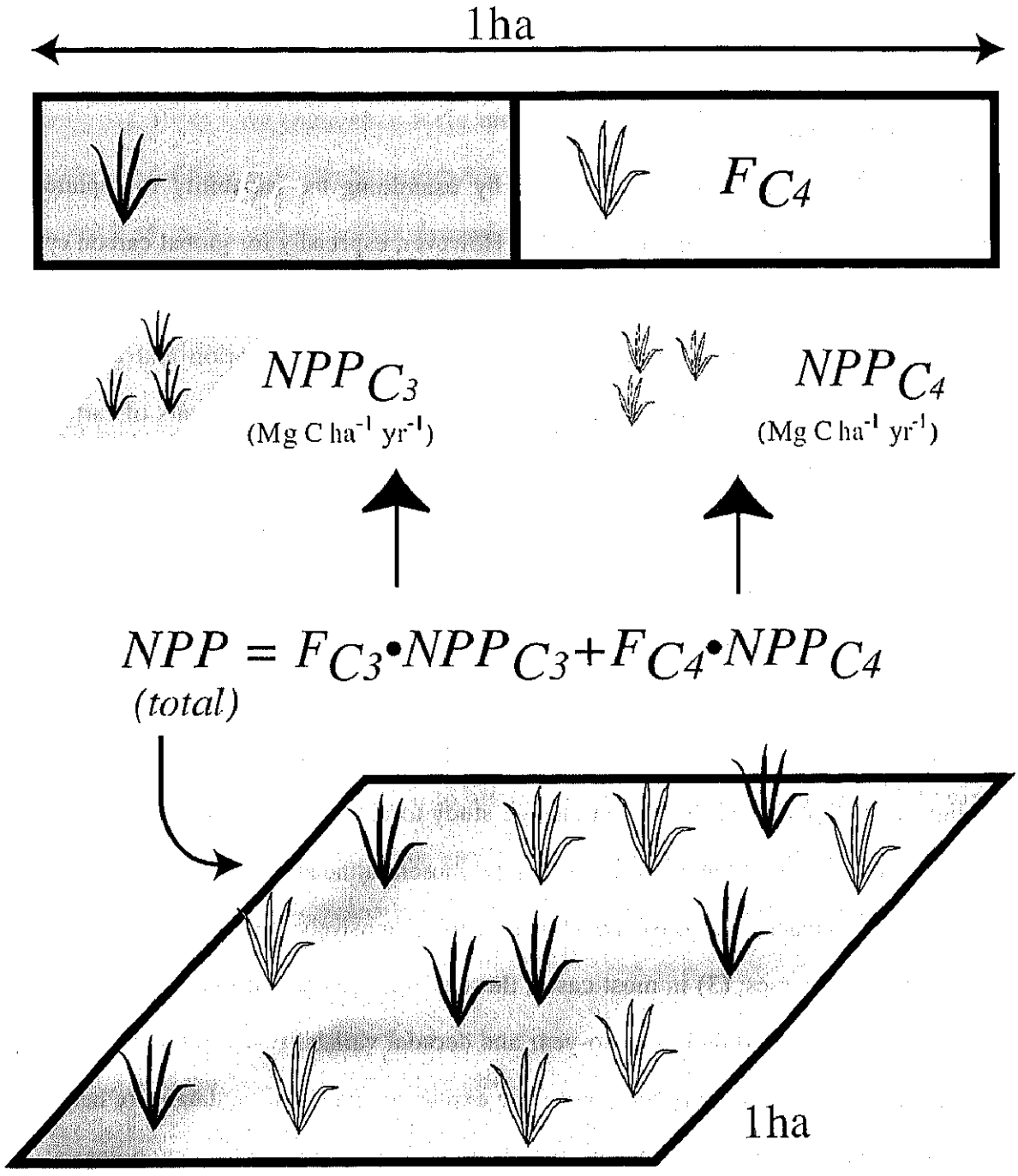

Fig. 2-31. Calculation of a C3-C4 mixed grassland ecosystem. An example of *NPP* is shown.